Advances in Differential Equations Volume 11, Number 2 (2006), 121–166

COMPARISONS BETWEEN THE BBM EQUATION AND A BOUSSINESQ SYSTEM

A.A. Alazman[1], J.P. Albert
Department of Mathematics, University of Oklahoma, Norman, OK 73019

J. L. Bona
Department of Mathematics, Statistics and Computer Science
University of Illinois at Chicago, Chicago, IL, 60607

M. Chen
Department of Mathematics, Purdue University, West Lafayette, IN 47907

J. Wu
Department of Mathematics, Oklahoma State University, Stillwater, OK 74078

(Submitted by: Reza Aftabizadeh)

Abstract. This project aims to cast light on a Boussinesq system of equations modelling two-way propagation of surface waves. Included in the study are existence results, comparisons between the Boussinesq equations and other wave models, and several numerical simulations. The existence theory is in fact a local well-posedness result that becomes global when the solution satisfies a practically reasonable constraint. The comparison result is concerned with initial velocities and wave profiles that correspond to unidirectional propagation. In this circumstance, it is shown that the solution of the Boussinesq system is very well approximated by an associated solution of the KdV or BBM equation over a long time scale of order $\frac{1}{\epsilon}$, where ϵ is the ratio of the maximum wave amplitude to the undisturbed depth of the liquid. This result confirms earlier numerical simulations and suggests further numerical experiments, some of which are reported here. Our results are related to recent results of Bona, Colin and Lannes [11] comparing Boussinesq systems of equations to the full two-dimensional Euler equations (see also the recent work of Schneider and Wayne [26] and Wright [30]).

Accepted for publication: September 2005.
AMS Subject Classifications: 35Q35, 35Q51, 35Q53, 65R20, 76B03, 76B07, 76B15, 76B25.

[1]College of Sciences, Department of Mathematics, King Saud University, Riyadh, 11451, Saudi Arabia

1. Introduction

In this report, attention will be directed to a Boussinesq system of partial differential equations,

$$\begin{aligned} &\eta_t + v_x + \epsilon(\eta v)_x - \tfrac{1}{6}\epsilon\eta_{xxt} = 0, \\ &v_t + \eta_x + \epsilon v v_x - \tfrac{1}{6}\epsilon v_{xxt} = 0, \end{aligned} \tag{1.1}$$

posed for $(x,t) \in \mathbb{R} \times \mathbb{R}^+$, with prescribed initial data

$$\eta(x,0) \,=\, \eta_0(x), \quad v(x,0) = v_0(x), \quad x \in \mathbb{R}. \tag{1.2}$$

The system (1.1) is a model equation for surface waves in a uniform horizontal channel filled with an irrotational, incompressible and inviscid liquid under the influence of gravity. These equations are considerably simpler than the full Euler equations,

$$\begin{aligned} \epsilon\phi_{xx} + S\phi_{yy} &= 0 \qquad \text{in } \{0 < y < 1 + \epsilon\eta(x,t)\}, \\ \phi_t + \tfrac{1}{2}\left(\epsilon\phi_x^2 + S\phi_y^2\right) + \eta &= 0 \qquad \text{on } \{y = 1 + \epsilon\eta(x,t)\}, \\ \eta_t + \epsilon\phi_x\eta_x - \frac{S}{\epsilon}\phi_y &= 0 \qquad \text{on } \{y = 1 + \epsilon\eta(x,t)\}, \\ \phi_y &= 0 \qquad \text{on } \{y = 0\}, \end{aligned} \tag{1.3}$$

for two-dimensional water waves in a channel with a flat bottom. Here the independent variable x determines position along the channel, y is the vertical coordinate, and t is proportional to elapsed time. The dependent variable $\phi = \phi(x,y,t)$ is the velocity potential (so $\nabla\phi$ is the velocity field), and the dependent variable $\eta = \eta(x,t)$ represents the vertical deviation of the free surface from its rest position at the point x at time t. The equations have been non-dimensionalized by scaling the variables: x is scaled by λ, a representative wave length; y is scaled by h_0, the undisturbed water depth; t is scaled by λ/c_0, where $c_0 = \sqrt{gh_0}$ with g being the acceleration of gravity; η is scaled by a, a representative wave amplitude; and ϕ is scaled by $ga\lambda/c_0$. The non-dimensional parameters ϵ and S (the Stokes number) are defined by $\epsilon = a/h_0$ and $S = a\lambda^2/h_0^3$.

The system (1.1) can be derived from (1.3) via a formal asymptotic expansion under the assumptions that ϵ is small and that S is of order one. (In fact, for purposes of notational convenience, in writing (1.1) the value of S has been set exactly equal to one; had S been allowed to take more general values, both occurrences of the constant $\frac{1}{6}$ in (1.1) would have been replaced by $\frac{1}{6}S$. In the remainder of this paper the assumption that $S = 1$ will remain in force whenever reference is made to the system (1.3).) These

assumptions on ϵ and S correspond to the physical assumptions that the waves being modelled have small amplitude and long wavelength relative to the water depth, with the condition $S \sim 1$ corresponding to a certain balance obtaining between the nonlinear effects owing to small but not infinitesimal amplitudes and frequency dispersion coming from large, but finite wavelengths. The variables x, y, t, and η in (1.1) retain the same interpretations as in (1.3); and the new independent variable $v(x,t)$ is the horizontal velocity of the fluid at the point $(x,y) = (x, \sqrt{2/3})$, scaled by the factor ag/c_0. That is, v represents the horizontal velocity at points whose distance from the channel bottom is $\sqrt{2/3}$ times the depth of the undisturbed fluid. This choice of variable v is, as explained in Bona, Chen and Saut [9, 10], related to the particular form which (1.1) takes, in opposition to other Boussinesq systems which are formally equivalent to (1.3) but which may have different mathematical properties.

One way in which (1.1) differs from other Boussinesq systems is that it is easier to integrate numerically. This fact was exploited in an earlier study [8], where numerical approximations of solutions of (1.1) were used to explore such phenomena as collisions between solitary waves which move in opposite directions. It was also observed in [8] that (1.1) has solitary-wave solutions that closely resemble solitary-wave solutions of the BBM equation

$$q_t + q_x + \tfrac{3}{2}\epsilon q q_x - \tfrac{1}{6}\epsilon q_{xxt} = 0. \tag{1.4}$$

For discussions of solitary-wave solutions of (1.1) and other Boussinesq systems, see [6, 19, 27, 28].

Equation (1.4), like the system (1.1), is a model equation for long, small-amplitude water waves; but has been simplified further through the assumption that the waves being modelled propagate only in one direction. It is therefore to be expected that the solitary-wave solutions of (1.1), being purely unidirectional, should resemble those of (1.4). It is the purpose of this paper to establish a similar correspondence between more general solutions of (1.1) and (1.4).

Below, a result is obtained showing that if the motion in the channel is properly initiated, then the solution of the Boussinesq system (1.1)-(1.2) exists and is tracked by a directly associated solution of the BBM equation (1.4) over the long time scale $\frac{1}{\epsilon}$. More precisely, it is shown that if $g(x)$ is a given initial wave profile, then if we consider the BBM equation (1.4) with initial value g and the Boussinesq system (1.1) with initial values

$$\eta(x,0) = g(x), \qquad v(x,0) = g(x) - \tfrac{1}{4}\epsilon g(x)^2,$$

then

$$|\eta - q| = O(\epsilon^2 t) \quad \text{and} \quad \left|v - \left(q - \tfrac{1}{4}\epsilon q^2\right)\right| = O(\epsilon^2 t)$$

at least for t of order $\frac{1}{\epsilon}$. As explained in [2], [11] and [14] for example, all the dependent variables η, q and v are of order one, so this result shows that at time $t = O(\frac{1}{\epsilon})$, the difference between η and q (and between v and $q - \frac{1}{4}\epsilon q^2$) lies at the order that can be attributed to the neglected terms in the approximation. Thus, at the theoretical level, one should not distinguish between (1.1) and (1.4) provided waves that are moving sensibly in one direction are in question. This theoretical result has its roots in the Ph.D. thesis of Alazman [1], directed by Albert at the University of Oklahoma.

In light of the work of Bona, Pritchard, and Scott [14] comparing solutions of the BBM equation (1.4) to solutions of the KdV equation

$$r_t + r_x + \tfrac{3}{2}\epsilon r r_x + \tfrac{1}{6}\epsilon r_{xxx} = 0, \tag{1.5}$$

our result is equivalent to a comparison between solutions of (1.1) and (1.5) (see Theorems 3.1 and 3.4 below). It is also closely related to recent results of Bona, Colin and Lannes [11] comparing solutions of the KdV equation and Boussinesq-type systems to solutions of the two-dimensional Euler equations (1.3) (see also Craig [21], Schneider and Wayne [26], and Wright [29, 30]).

Our analysis begins with a study of the well-posedness of the initial-value problem (1.1)-(1.2). An informal interpretation of the principal well-posedness result is that as long as the channel bed does not run dry, the solution continues to exist. A technical description of this result will appear in Section 2.

The statement of the main comparison result is given at the beginning of Section 3, along with a discussion of the related comparison results mentioned above. The remainder of Section 3 contains a detailed proof of the main result.

The theory developed in Section 3 motivates several accurate numerical experiments whose outcomes are reported in Section 4. They further illuminate the relation between the Boussinesq system and the BBM equation. In particular, some of the comparisons exhibited are quite startling.

The paper closes with a brief conclusion which provides an appreciation of the present development and indications of interesting related lines of investigation.

2. Well-posedness results

We begin with a précis of the notation to be used in the technical sections of the paper. For $1 \leq p < \infty$, L_p denotes the space of equivalence classes of

Lebesgue measurable, p^{th}-power integrable, real-valued functions defined on the real line $\mathbb{R}$. The usual modification is in effect for $p = \infty$. The norm on L_p is written as $\|\cdot\|_{L_p}$. For $f \in L_2$, the Fourier transform $\widehat{f}$ of f is defined as

$$\widehat{f}(k) = \int_{-\infty}^{\infty} e^{-ikx} f(x)\, dx.$$

For $s \geq 0$, the L_2-based Sobolev class H^s is the subspace of those L_2 functions whose derivatives up to order s all lie in L_2, and the norm on H^s is taken to be

$$\|f\|_s^2 = \int_{-\infty}^{\infty} (1 + k^2)^s |\widehat{f}(k)|^2\, dk.$$

For non-negative integers m, C_b^m is the space of m-times continuously differentiable, real-valued functions defined on $\mathbb{R}$ whose derivatives up to order m are bounded on $\mathbb{R}$. The norm is

$$\|f\|_{C_b^m} = \sup_{x \in \mathbb{R}} \sum_{0 \leq j \leq m} |f^{(j)}(x)|.$$

For any Banach space X and real number $T > 0$, $C(0, T; X)$ is the class of continuous functions from $[0, T]$ to X. If $X = L_2$, we write $\mathcal{L}_T$ for $C(0, T; L_2)$. Similarly, we write $\mathcal{B}_T^k$ for $C(0, T; C_b^k)$ and $\mathcal{H}_T^k$ for $C(0, T; H^k)$, $k = 1, 2, \ldots$. Of course, $\mathcal{H}_T^0 = \mathcal{L}_T$. If X and Y are Banach spaces, then their Cartesian product $X \times Y$ is a Banach space with a product norm defined by $\|(f, g)\|_{X \times Y} = \|f\|_X + \|g\|_Y$.

Attention is now turned to the well-posedness theory. The principal result is the following.

Theorem 2.1. *(i) Let $(\eta_0, v_0) \in H^k \times H^k$, where $k \geq 0$. Then there exists $T > 0$, depending only on $\|(\eta_0, v_0)\|_{H^k \times H^k}$, and a unique solution pair $(\eta, v) \in \mathcal{H}_T^k \times \mathcal{H}_T^k$ for the system of integral equations (2.2) below. For any $k \geq 0$, (η, v) comprises a distributional solution of the initial-value problem (1.1)–(1.2). If $k \geq 2$, then (η, v) is a classical solution of (1.1)–(1.2). The mapping that associates to initial data the corresponding solution of (2.2) is uniformly Lipschitz continuous on any bounded subset of $H^k \times H^k$.*

(ii) The conclusions of (i) still hold if H^k is replaced by C_b^m, where $m \geq 0$, and $\mathcal{H}_T^k$ is replaced by $\mathcal{B}_T^m$. In this case, (η, v) is a classical solution of (1.1)–(1.2) if $m \geq 1$.

(iii) Let $T_0 \in (0, \infty]$ be the maximal existence time for the solution described in (i); i.e., T_0 is the supremum of the set of values of T such that the solution exists on the interval $[0, T]$. If there exist numbers $\alpha > 0$ and

$a < T_0$ such that $1 + \epsilon\eta(x,t) > \alpha$ for all $x \in \mathbb{R}$ and all $t \in (a, T_0)$, then $T_0 = \infty$. Also, if there exist numbers $M \in \mathbb{R}$ and $a \in \mathbb{R}$ such that

$$\|(\eta(\cdot,t), v(\cdot,t))\|_{L_2\times L_2} \leq M$$

for all $t \in (a, T_0)$, then $T_0 = \infty$.

Remark 2.2. It is worth emphasis that Theorem 2.1 is a local well-posedness result, not a global theorem. The criteria in (iii) provide sufficient conditions for solutions to be global. It seems likely that for ϵ small, initial data that is of order one will develop into globally defined solutions. However, numerical simulations not reported here suggest that large data may lead to solutions that form singularities in finite time. Both the criteria in (iii) are more than plausible; indeed, any physically relevant solution will certainly satisfy both these conditions. In particular, the condition $1 + \epsilon\eta > 0$, when interpreted in the original physical variables, means simply that the total water height does not reach zero, which is to say the channel does not become dry.

The proof of Theorem 2.1 is similar to the proofs given for analogous results in [3], [8] and [10]. The details are therefore only sketched. Certain aspects of the proof offered below reappear in Section 3 in the proof of the main comparison result.

To begin, write the system (1.1) in the form

$$\begin{aligned}\left(1 - \tfrac{1}{6}\epsilon\partial_x^2\right)\eta_t &= -\left(v(1+\epsilon\eta)\right)_x,\\ \left(1 - \tfrac{1}{6}\epsilon\partial_x^2\right)v_t &= -\left(\eta + \tfrac{\epsilon}{2}v^2\right)_x.\end{aligned}$$

Inverting the operator $\left(1 - \frac{1}{6}\epsilon\partial_x^2\right)$ subject to zero boundary conditions at infinity leads to the relations

$$\begin{aligned}\eta_t &= \mathcal{M}_\epsilon * (v(1+\epsilon\eta))_x,\\ v_t &= \mathcal{M}_\epsilon * \left(\eta + \tfrac{\epsilon}{2}v^2\right)_x,\end{aligned} \tag{2.1}$$

where the kernel $\mathcal{M}_\epsilon$ is defined via its Fourier transform, *viz.*,

$$\widehat{\mathcal{M}_\epsilon}(k) = -\Big(\frac{1}{1+\epsilon k^2/6}\Big).$$

Direct calculation using the Residue Theorem shows that for $x \in \mathbb{R}$,

$$\mathcal{M}_\epsilon(x) = -\frac{1}{2}\sqrt{\frac{6}{\epsilon}}e^{-\sqrt{6/\epsilon}|x|}.$$

Integrating by parts in (2.1) and then integrating with respect to t over the interval $(0,t)$ yields

$$\begin{aligned} \eta(x,t) &= \eta_0(x) + \int_0^t \mathcal{K}_\epsilon * (v(1+\epsilon\eta))\, d\tau, \\ v(x,t) &= v_0(x) + \int_0^t \mathcal{K}_\epsilon * \left(\eta + \frac{\epsilon}{2}v^2\right) d\tau \end{aligned} \tag{2.2}$$

where

$$\mathcal{K}_\epsilon = \frac{3}{\epsilon}(\operatorname{sgn} x)e^{-\sqrt{6/\epsilon}|x|} \quad \text{and} \quad \widehat{\mathcal{K}_\epsilon}(k) = \frac{-ik}{1+\epsilon k^2/6}.$$

The following technical lemma about the action of convolution with $\mathcal{K}_\epsilon$ and $\mathcal{M}_\epsilon$ will be used immediately and later on as well. Their proof involves elementary considerations which are here omitted.

Lemma 2.3. *There are constants C independent of f, g and $\epsilon > 0$ such that the following inequalities hold. For any $s \geq 0$,*

$$\|\mathcal{K}_\epsilon * f\|_s \leq C\epsilon^{-\frac{1}{2}}\|f\|_s, \tag{2.3}$$

$$\|\mathcal{K}_\epsilon * f\|_s \leq C\|f\|_{s+1},$$

$$\|\mathcal{K}_\epsilon * f\|_{s+1} \leq C\epsilon^{-1}\|f\|_s,$$

$$\|\mathcal{K}_\epsilon * (fg)\|_{L_2} \leq C\epsilon^{-3/4}\|f\|_{L_2}\|g\|_{L_2}, \tag{2.4}$$

$$\|\mathcal{M}_\epsilon * f\|_s \leq C\|f\|_s. \tag{2.5}$$

For any integer $m \geq 0$,

$$\|\mathcal{K}_\epsilon * f\|_{C_b^m} \leq C\epsilon^{-\frac{1}{2}}\|f\|_{C_b^m}, \tag{2.6}$$

$$\|\mathcal{K}_\epsilon * (fg)\|_{C_b^m} \leq C\epsilon^{-\frac{1}{2}}\|f\|_{C_b^m}\|g\|_{C_b^m}. \tag{2.7}$$

The proof of part (i) of Theorem 2.1 will now be considered. Let $T > 0$ be arbitrary for the moment, and write the pair of integral equations (2.2) symbolically as $(\eta, v) = A(\eta, v)$. Here A is the obvious mapping of functions with domain $\mathbb{R} \times [0,T]$ defined by the right-hand side of (2.2). It will be shown that the mapping A is contractive on a suitable subset of $\mathcal{L}_T \times \mathcal{L}_T$. Indeed, take any two elements (η_1, v_1) and (η_2, v_2) from $\mathcal{L}_T \times \mathcal{L}_T$, and notice that

$$\begin{aligned} \|A(\eta_1,v_1) - A(\eta_2,v_2)\|_{\mathcal{L}_T\times\mathcal{L}_T} &= \left\| \int_0^t \mathcal{K}_\epsilon * (v_1 - v_2 + \epsilon(\eta_1 v_1 - \eta_2 v_2))d\tau \right\|_{\mathcal{L}_T} \\ &\quad + \left\| \int_0^t \mathcal{K}_\epsilon * (\eta_1 - \eta_2 + \frac{1}{2}\epsilon(v_1^2 - v_2^2))d\tau \right\|_{\mathcal{L}_T}. \end{aligned}$$

Apply the basic estimates in Lemma 2.3 to derive the inequality

$$\begin{aligned}
&\|A(\eta_1,v_1)-A(\eta_2,v_2)\|_{\mathcal{L}_T\times\mathcal{L}_T}\\
&\le CT\Big[\epsilon^{-\frac{1}{2}}\|v_1-v_2\|_{\mathcal{L}_T}+\epsilon^{\frac{1}{4}}(\|\eta_1-\eta_2\|_{\mathcal{L}_T}\|v_1\|_{\mathcal{L}_T}+\|\eta_2\|_{\mathcal{L}_T}\|v_1-v_2\|_{\mathcal{L}_T})\Big]\\
&\quad+CT\Big[\epsilon^{-\frac{1}{2}}\|\eta_1-\eta_2\|_{\mathcal{L}_T}+\epsilon^{\frac{1}{4}}(\|v_1\|_{\mathcal{L}_T}+\|v_2\|_{\mathcal{L}_T})\|v_1-v_2\|_{\mathcal{L}_T}\Big]\\
&\le CT\epsilon^{-\frac{1}{2}}\Big[1+\|(\eta_1,v_1)\|_{\mathcal{L}_T\times\mathcal{L}_T}+\|(\eta_2,v_2)\|_{\mathcal{L}_T\times\mathcal{L}_T}\Big]\\
&\qquad\qquad\times\|(\eta_1,v_1)-(\eta_2,v_2)\|_{\mathcal{L}_T\times\mathcal{L}_T}.
\end{aligned}$$

Suppose that both (η_1,v_1) and (η_2,v_2) are in the closed ball B_R of radius R about the zero function in $\mathcal{L}_T\times\mathcal{L}_T$. Then, the last estimate leads to the inequality

$$\|A(\eta_1,v_1)-A(\eta_2,v_2)\|_{\mathcal{L}_T\times\mathcal{L}_T}\le\Theta\|(\eta_1,v_1)-(\eta_2,v_2)\|_{\mathcal{L}_T\times\mathcal{L}_T},\tag{2.8}$$

where $\Theta=CT\epsilon^{-\frac{1}{2}}(1+2R)$. If $\Theta<1$ and A maps B_R to itself, then the hypothesis of the contraction mapping theorem will be satisfied. By application of (2.8),

$$\|A(\eta,v)\|_{\mathcal{L}_T\times\mathcal{L}_T}\le\Theta\|(\eta,v)\|_{\mathcal{L}_T\times\mathcal{L}_T}+\|\eta_0\|_{L_2}+\|v_0\|_{L_2}\le\Theta R+b.$$

Thus, if $b\le(1-\Theta)R$, then A maps B_R to itself. Choosing $R=2b$ and $T=\frac{C}{2}\epsilon^{\frac{1}{2}}(1+2R)^{-1}$ gives a closed set B_R in $\mathcal{L}_T\times\mathcal{L}_T$ on which A is a contractive self map. This proves existence in $\mathcal{L}_T\times\mathcal{L}_T$ for some $T>0$.

Next, observe that from Lemma 2.3 if $f\in H^s$, then $\mathcal{K}_\epsilon*f\in H^{s+1}$. Therefore a standard bootstrap type argument allows one to conclude that if (2.2) has a solution in $\mathcal{L}_T\times\mathcal{L}_T$ whose initial data happens to lie in $H^s\times H^s$, then this solution is in fact in $\mathcal{H}^s_T\times\mathcal{H}^s_T$. Moreover, the continuity of the solution map follows easily from the simple dependence of the operator A on the initial data. Indeed, further analysis shows that the solution map is analytic.

The question of uniqueness is now considered. Let (η_1,v_1) and (η_2,v_2) be two solutions of (2.2) in $\mathcal{L}_T\times\mathcal{L}_T$, and let $(\eta,v)=(\eta_1,v_1)-(\eta_2,v_2)$. The pair (η,v) satisfies the integral equations

$$\begin{aligned}
\eta&=\int_0^t\mathcal{K}_\epsilon*(v_1-v_2+\epsilon(\eta_1v_1-\eta_2v_2))\,d\tau,\\
v&=\int_0^t\mathcal{K}_\epsilon*(\eta_1-\eta_2+\frac{1}{2}\epsilon(v_1^2-v_2^2))\,d\tau.
\end{aligned}$$

As in the proof of the existence result, the following estimate obtains:

$$\|(\eta,v)\|_{L_2\times L_2} \le C\epsilon^{-\frac{1}{2}}\int_0^t \Big[1+\|(\eta_1,v_1)\|_{L_2\times L_2}+\|(\eta_2,v_2)\|_{L_2\times L_2}\Big]\cdot \times \|(\eta_1,v_1)-(\eta_2,v_2)\|_{L_2\times L_2}\,d\tau$$
$$\le D\int_0^t \|(\eta,v)\|_{L_2\times L_2}\,d\tau,$$

where D is independent of $t\in[0,T]$. Gronwall's Lemma then implies that $\eta=0$ and $v=0$ on $[0,T]$, so proving uniqueness. The proof of part (i) of the Theorem is now complete.

For part (ii), we merely note that in view of (2.6) and (2.7), the same contraction-mapping argument yields local existence for initial data in C_b^m, and the same uniqueness and bootstrapping argument applies as well.

The global existence result stated in part (iii) of Theorem 2.1 depends on the invariance of the functional

$$E(t)=E(\eta,v,t)=\int_{-\infty}^{\infty}\left[\eta^2+(1+\epsilon\eta)v^2\right]\,dx.$$

Lemma 2.4. *Let (η,v) be a solution pair of the initial-value problem* (1.1), (1.2) *in $\mathcal{H}_T^s\times\mathcal{H}_T^s$, for some $s\ge\frac{1}{6}$. Then $E(t)=E(0)$ for all $t\in[0,T]$.*

Proof. Assume first that (η,v) is sufficiently regular for the following formal calculations to be valid; say, $(\eta,v)\in(\mathcal{H}_T^1\times\mathcal{H}_T^1)\cap(\mathcal{B}_T^3\times\mathcal{B}_T^3)$. Multiply the first equation in (1.1) by $(\eta+\frac{1}{2}\epsilon v^2-\frac{1}{6}\epsilon v_{xt})$ and the second by $(v+\epsilon v\eta-\frac{1}{6}\epsilon\eta_{xt})$, add them, and integrate with respect to x to reach the relation

$$\int_{-\infty}^{\infty}\Big(\eta_t\Big[\eta+\frac{\epsilon}{2}v^2-\frac{1}{6}\epsilon v_{xt}\Big]+v_t\Big[v+\epsilon v\eta-\frac{1}{6}\epsilon\eta_{xt}\Big]\Big)dx$$
$$=-\int_{-\infty}^{\infty}\Big(\Big[\eta+\frac{\epsilon}{2}v^2-\frac{1}{6}\epsilon v_{xt}\Big]\Big[v+\epsilon v\eta-\frac{1}{6}\epsilon=\eta_{xt}\Big]\Big)_x dx=0.$$

Regroup the terms on the left-hand side to obtain

$$\int_{-\infty}^{\infty}\Big(\frac{1}{2}\left[\eta^2+(1+\epsilon\eta)v^2\right]_t-\frac{1}{6}\epsilon\left[\eta_t v_{xt}+v_t\eta_{xt}\right]\Big)dx=0. \tag{2.9}$$

Since

$$\int_{-\infty}^{\infty}\left[\eta_t v_{xt}+v_t\eta_{xt}\right]dx=\int_{-\infty}^{\infty}(\eta_t v_t)_x\,dx=0,$$

it follows from (2.9) that

$$\frac{d}{dt}\int_{-\infty}^{\infty}\left[\eta^2+(1+\epsilon\eta)v^2\right]dx=0,$$

and hence $E(t) = E(0)$ for all $t \in [0, T]$.

Now suppose that (η, v) is, say, a solution in $\mathcal{H}^s_T \times \mathcal{H}^s_T$ with $s \geq \frac{1}{6}$. We can approximate (η_0, v_0) by regular initial data (η_{0j}, v_{0j}) and thus obtain solutions (η_j, v_j) on $[0, T]$ to which the above calculation applies, and which, by Theorem 2.1(i), approximate (η, v) in $\mathcal{H}^s_T \times \mathcal{H}^s_T$. Moreover, since H^s is continuously embedded in L_3 by the Sobolev embedding theorem, then (η_j, v_j) also approximates (η, v) in $C(0, T; L_3) \times C(0, T; L_3)$. The desired result then follows by passing to the limit as $j \to \infty$.

Remark 2.5. The functional E, together with the functional

$$F(t) = F(\eta, v, t) = \int_{-\infty}^{\infty} \left[\eta v + \frac{\epsilon}{6}\eta_x v_x\right] dx,$$

and the obvious conserved quantities

$$\int_{-\infty}^{\infty} \eta \; dx \quad \text{and} \quad \int_{-\infty}^{\infty} v \; dx$$

comprise the only known invariants for the system (1.1). Note that one obtains the invariance of F by multiplying the first equation in (1.1) by v and the second equation in (1.1) by η, adding the results, and integrating with respect to x.

The simple idea exposed in the proof of Lemma 2.4 can also be used to obtain an invariant for a more general type of Boussinesq system.

Corollary 2.6. *Consider the following four parameter class of model equations*

$$\eta_t + u_x + (u\eta)_x + au_{xxx} - b\eta_{xxt} = 0$$

and

$$u_t + \eta_x + uu_x + c\eta_{xxx} - du_{xxt} = 0.$$

If $b = d$, then for sufficiently regular solutions (η, u), the quantity

$$G(t) = \int_{-\infty}^{\infty} \left[\eta^2 + (1 + \eta)u^2 - c\eta_x^2 - au_x^2\right] dx$$

is invariant, i.e., $G(t) = G(0)$ for all $t \geq 0$.

Remark 2.7. This class of model equations was put forward by Bona, Chen and Saut [9], [10] as approximations of the two-dimensional free surface Euler equations for the motion of an ideal, incompressible liquid. In this context, a, b, c and d are not independently specifiable parameters. This class of equations reappears briefly in the next section (see Theorem 3.7).

The proof of part (iii) of Theorem 2.1 now proceeds by means of the usual continuation-type argument, as follows. Suppose $s > \frac{1}{2}$ so that $\eta(\cdot,t) \in C_b(\mathbb{R})$ for all t during which the solution exists, and that $1+\epsilon\eta > \alpha > 0$ for all $x \in \mathbb{R}$ and all $t \in (a, T_0)$. According to Lemma 2.4, for $\beta = \max\{1, \alpha^{-1}\}$, we have

$$\|\eta(\cdot,t)\|_{L_2}^2 + \|v(\cdot,t)\|_{L_2}^2 = \int_{-\infty}^{\infty} (\eta(\cdot,t)^2 + v(\cdot,t)^2)\, dx \le \beta E(t) = \beta E(0)$$

for all $t \in (a, T_0)$. Now the local existence result stated in part (i) of the Theorem implies that if (1.1) is posed with initial data $(\eta(t_0), v(t_0))$ satisfying

$$\|\eta(t_0)\|_{L_2}^2 + \|v(t_0)\|_{L_2}^2 \le \beta E(0),$$

then a solution persists in $L_2 \times L_2$ on the time interval $(t_0, t_0 + 2\delta)$, where δ depends only on $\beta E(0)$. If $T_0 < \infty$, one can choose t_0 such that $T_0 > t_0 > \min(a, T_0 - \delta)$, and thereby obtain an extension of the solution to $[0, t_0 + \delta)$. A bootstrap argument then immediately yields that this solution is in fact in $\mathcal{H}^s_{t_0+\delta} \times \mathcal{H}^s_{t_0+\delta}$. But this contradicts the maximality of T_0. Hence we must have $T_0 = \infty$. Obviously, the same argument also shows that $T_0 = \infty$ under the assumption that $\|(\eta, v)\|_{L_2 \times L_2}$ remains bounded near T_0.

3. The Comparison Results

It was shown in [3] that the BBM equation (1.4) with initial condition $q(x,0) = g(x)$ has a unique global solution $q \in C([0,\infty), H^s)$ if $g \in H^s$ with $s \ge 1$. Moreover, for each $T > 0$, the correspondence $g \mapsto q$ is an analytic mapping of H^s to $C([0,T]; H^s)$ while, if $l > 0$, the correspondence $g \mapsto \partial_t^l q$ is an analytic mapping of H^s to $C([0,T]; H^{s+1})$. This result was recently improved to include the range $s \ge 0$ in [17].

In this section we consider the circumstances under which solutions of the Boussinesq system (1.1) can be approximated using appropriate solutions of the BBM equation (1.4). More precisely, conditions on the initial data (η_0, v_0) are determined which guarantee that (1.1) will generate a solution (η, v) in which η is well tracked by the solution q of the (1.4) with initial data $q(x,0) = \eta_0$.

At the lowest order, we expect that if $\eta_0 = v_0$, then the wave described by (η, v) moves mainly in one direction (see the discussion in [5]). However, the analysis in the last-quoted reference suggests that this simple imposition of initial data for (1.1) would not yield a solution which agrees closely with that of the BBM equation on the time scale over which nonlinearity and dispersion can have an order-one relative effect on the wave profile. Rather,

one expects to have to correct the lowest-order approximation of the relation between amplitude and velocity at higher order to see the Boussinesq system evincing unidirectional propagation over such a long time interval. As shown below in Theorem 3.1, this is indeed the case, and the appropriate relation between the initial amplitude and velocity is

$$\eta(x,0) = g(x) \quad \text{and} \quad v(x,0) = g(x) - \frac{1}{4}\epsilon g(x)^2. \tag{3.1}$$

3.1. **Discussion of the main results.** The principal new outcome of our analysis is summarized in the first theorem.

Theorem 3.1. *Let $j \geq 0$ be an integer. Then for every $K > 0$, there exist constants C and D depending on K such that the following is true. Suppose $g \in H^{j+5}$ with $\|g\|_{j+5} \leq K$. Let (η, v) be the solution of the Boussinesq system* (1.1)*, with initial data defined by* (3.1)*, and let q be the solution of the BBM equation* (1.4) *with initial data $q(x,0) = g(x)$. Define w by*

$$w = q - \tfrac{1}{4}\epsilon q^2. \tag{3.2}$$

Then for all $\epsilon \in (0,1]$, if

$$0 \leq t \leq T = D\epsilon^{-1}, \tag{3.3}$$

then

$$\|\eta(\cdot,t) - q(\cdot,t)\|_j + \|v(\cdot,t) - w(\cdot,t)\|_j \leq C\epsilon^2 t. \tag{3.4}$$

Notice that included as part of Theorem 3.1 is the assertion that the Boussinesq system has a solution in $\mathcal{H}^j_T \times \mathcal{H}^j_T$ for T at least as large as D/ϵ.

When combined with the basic inequality

$$\|f\|_{C_b(\mathbb{R})} \leq \|f\|^{\frac{1}{2}}_{L_2(\mathbb{R})} \|f'\|^{\frac{1}{2}}_{L_2(\mathbb{R})},$$

valid for any $f \in H^1(\mathbb{R})$, Theorem 3.1 yields the following.

Corollary 3.2. *Let $s \geq 6$ and $j \in [0, s-6]$ both be integers. Then for every $K > 0$, there exist constants C and D such that the following is true. Suppose $g \in H^s$ with $\|g\|_s \leq K$. Let (η, v) be a solution of the Boussinesq system* (1.1)*, with initial data* (1.2) *defined by* (3.1)*; let q be the solution of the BBM equation* (1.4) *with $q(x,0) = g(x)$; and let w be defined by* (3.2)*. Then for all $\epsilon \in (0,1]$, if $0 \leq t \leq T = D\epsilon^{-1}$, then*

$$\|\partial_x^j(\eta - q)(\cdot,t)\|_{C_b(\mathbb{R})} + \|\partial_x^j(v - w)(\cdot,t)\|_{C_b(\mathbb{R})} \leq C\epsilon^2 t.$$

Remark 3.3. This result shows that, under the stated restrictions on the initial data for (1.1), solutions of (1.1) and (1.4) agree with each other to an accuracy equaling the size of the terms which were ignored in deriving (1.1) as model equations from the Euler equations. The comparison is shown to hold on a time scale of order $1/\epsilon$, which is long enough for nonlinear and dispersive effects to have an order-one influence on the wave form.

The proof of Theorem 3.1 is conveniently made by a slightly indirect argument. Indeed, thus far we have focused on the BBM equation as a model for unidirectional surface waves because it lends itself easily to the numerical investigations described below in Section 4. However, one could equally well initiate this discussion using the KdV equation (1.5) as the model for unidirectional surface waves. The two equations KdV and BBM are in fact formally equivalent models in the Boussinesq regime, and, indeed, there is a similar type of comparison result already available between their solutions. Here is the KdV version of Theorem 3.1.

Theorem 3.4. *Let $j \geq 0$ be an integer. Then for every $K > 0$, there exist constants C and D such that the following is true. Suppose $g \in H^{j+5}$ with $\|g\|_{j+5} \leq K$. Let (η, v) be the solution of the Boussinesq system* (1.1)*, with initial data defined by* (3.1)*, and let r be the solution of the KdV equation* (1.5) *with initial data $r(x,0) = g(x)$. Define z by*

$$z = r - \tfrac{1}{4}\epsilon r^2. \tag{3.5}$$

For all $\epsilon \in (0,1]$, if $0 \leq t \leq T = D\epsilon^{-1}$, then

$$\|\eta(\cdot,t) - r(\cdot,t)\|_j + \|v(\cdot,t) - z(\cdot,t)\|_j \leq C\epsilon^2 t. \tag{3.6}$$

Implicit in the statement of the preceding theorem is the presumption that KdV is well-posed in H^s. Although the KdV well-posedness theory is somewhat more involved than that of BBM, global well-posedness of KdV in H^s has been proved for values of s down to $s = 0$ and below. See for example [16, 20, 24].

Once Theorem 3.4 has been proved, the final ingredient in the proof of Theorem 3.1 is the following result comparing solutions of (1.4) to those of (1.5).

Theorem 3.5. *Let $j \geq 0$ be an integer. Then for every $K > 0$ and every $D > 0$, there exists a constant $C > 0$ such that the following is true. Suppose $g \in H^{j+5}$ with $\|g\|_{j+5} \leq K$. Let q be the solution of the BBM equation* (1.4) *with initial data $q(x,0) = g(x)$ and let r be the solution of the KdV equation* (1.5) *with the same initial data $r(x,0) = g(x)$. Then for all $\epsilon \in (0,1]$, if*

$0 \le t \le T = D\epsilon^{-1}$, *then*

$$\|q(\cdot,t) - r(\cdot,t)\|_j \le C\epsilon^2 t. \tag{3.7}$$

Theorem 3.5 is taken from [14], where it is proved in a different form. For the reader's convenience we briefly sketch the proof of the present formulation in the Appendix.

Assuming that (3.6) and (3.7) hold on the requisite time scales, one immediately deduces the estimate on $\|\eta - q\|_j$ in (3.4) from the triangle inequality. The estimate on $\|v - w\|_j$ in (3.4) also follows easily from (3.6), (3.7), and the triangle inequality, once one takes into account the definitions of w and z and the fact that uniform bounds are available on $\|r\|_j$ (cf. Theorem A2 below). Hence, to complete the proof of Theorem 3.1, it remains only to prove Theorem 3.4. This is done below in Subsections 3.2 and 3.3.

We remark that it is also possible to prove a comparison result for (1.4) directly, without first proving Theorem 3.4. (See [1] for details. The result proved there is slightly less satisfactory and consequently we have preferred the present development.)

Theorems 3.1 and 3.4 are closely related to several other results [11, 21, 26, 29, 30] on long-wave approximations to solutions of the water-wave problem (1.3). In (1.3), let $u(x,t)$ denote the horizontal velocity of the fluid at the free surface, so that $u(x,t) = \phi_x(x, 1+\epsilon\eta(x,t), t)$. If $\eta(x,t)$ and $u(x,t)$ are known as functions of x for a given time t, then the velocity potential $\phi(x,y,t)$ within the fluid domain can be found by solving a standard elliptic boundary-value problem on the domain. Therefore the initial-value problem for the system (1.3) is equivalent to an initial-value problem for the functions $\eta(x,t)$ and $u(x,t)$.

The problem of relating the behavior of solutions (η, u) of the initial-value problem for (1.3) to general solutions of (1.5) on long time scales was first considered by Craig in [21]. Schneider and Wayne [26] improved Craig's existence theory and established that a large class of long-wave solutions of (1.3) are well approximated by combinations of solutions of an uncoupled system of two KdV equations, one for disturbances moving to the left and one for disturbances moving to the right. Bona, Colin and Lannes [11] and Wright [30] sharpened and extended the results of [26]. For example, we have the following result from [11].

Theorem 3.6. *Let $j \ge 0$ be an integer. Then for every $K > 0$ and $D > 0$, there exist constants $C > 0$ and $\epsilon_0 > 0$ such that the following is true. Suppose $g(x)$ and $h(x)$ are functions satisfying $\|(1+x^2)g(x)\|_J \le K$ and $\|(1+x^2)h(x)\|_J \le K$, where J is a sufficiently large number depending only*

on j. Let α be the solution of

$$\alpha_t + \alpha_x + \tfrac{3}{4}\epsilon\alpha\alpha_x + \tfrac{1}{6}\alpha_{xxx} = 0$$

with initial data $\alpha(x,0) = h(x) + g(x)$, and let β be the solution of

$$\beta_t - \beta_x + \tfrac{3}{4}\epsilon\beta\beta_x + \tfrac{1}{6}\beta_{xxx} = 0$$

with initial data $\beta(x,0) = h(x) - g(x)$. Let $\epsilon \in (0, \epsilon_0]$ be given, and let $T = D\epsilon^{-1}$. Then there exists a unique solution $(\tilde\eta, \tilde u)$ to (1.3) in the space $C(0,T; H^j \times H^{j-1/2})$ with initial data $\tilde\eta(x,0) = g(x)$ and $\tilde u(x,0) = h(x)$. Moreover, for all $t \in [0,T]$,

$$\|\tilde\eta(\cdot,t) - \tfrac{1}{2}\left(\alpha(\cdot,t) + \beta(\cdot,t)\right)\|_j + \|\tilde u(\cdot,t) - \tfrac{1}{2}\left(\alpha(\cdot,t) - \beta(\cdot,t)\right)\|_j \le C\epsilon^2 t. \quad (3.8)$$

In particular, if $g(x) = h(x)$, then we have

$$\|\tilde\eta(\cdot,t) - r(\cdot,t)\|_j + \|\tilde u(\cdot,t) - r(\cdot,t)\|_j \le C\epsilon^2 t \quad (3.9)$$

for all $t \in [0,T]$, where r is the solution of (1.5) with initial data $r(x,0) = g(x)$.

Proof. The general case of the theorem is a restatement of Theorem 5.1(i') of [11]. The particular case when $g(x) = h(x)$ follows as an immediate consequence, since then $\beta = 0$ and $r = \frac{1}{2}\alpha$. □

Remark 3.7. A comparison result similar to the above also follows from Theorem 1.3 and Corollary 1.5 of Schneider and Wayne [26] (but note that (1.11) in [26] contains a misprint: both the coefficients with value 3/4 should be emended to 3/2). Indeed, a perusal of p. 1492 of their argument shows that they prove an estimate which is somewhat stronger than the one they state, and which in our variables reads

$$\|\tilde\eta(\cdot,t) - \tfrac{1}{2}(\alpha(\cdot,t)+\beta(\cdot,t))\|_{C_b^{j-3/2}} + \|\tilde u(\cdot,t) - \tfrac{1}{2}(\alpha(\cdot,t)-\beta(\cdot,t))\|_{C_b^{j-3/2}} \le C\epsilon^{3/4}. \quad (3.10)$$

More recently, Wright [29, 30] has improved Schneider and Wayne's result by establishing a system of model equations for long-wave solutions of (1.3) which is accurate to order ϵ^2. (System (1.1) and equations (1.4) and (1.5) are, by contrast, only accurate to order ϵ.) It follows from Corollary 2 of [29] that the power $\epsilon^{3/4}$ in (3.10) can be increased to ϵ^1. This estimate coincides with (3.8) at $t = D\epsilon^{-1}$ but is weaker for smaller values of t. Both Wright's estimate and (3.8) are sharp in the sense that the powers of ϵ involved cannot be increased in general.

The theory of [11] goes beyond the approximation of (1.3) by KdV-type equations to include approximations by a variety of Boussinesq-type systems as well. As a particular consequence we obtain the following theorem.

Theorem 3.8. *Let $j \geq 0$ be an integer. Then for every $K > 0$ and $D > 0$, there exist constants $C > 0$ and $\epsilon_0 > 0$ such that the following is true. Suppose $g(x)$ and $h(x)$ are functions satisfying $\|(1+x^2)g(x)\|_J \leq K$ and $\|(1+x^2)h(x)\|_J \leq K$, where J is a sufficiently large number depending only on j. Let $\epsilon \in (0, \epsilon_0]$ be given, and let $T = D\epsilon^{-1}$. Then there exists a unique solution (η, v) of the Boussinesq system (1.1) in $\mathcal{H}^J_T \times \mathcal{H}^J_T$ with initial data given by $\eta(x,0) = g(x)$ and $v(x,0) = (1 - \frac{\epsilon}{6}\partial_x^2)^{-1}h(x)$. Moreover, if $(\tilde{\eta}, \tilde{u})$, α, β, and r are as defined in Theorem* 3.6, *then for all $t \in [0,T]$ we have*

$$\|\tilde{\eta}(\cdot,t) - \eta(\cdot,t)\|_j + \|\tilde{u}(\cdot,t) - (1 - \tfrac{\epsilon}{6}\partial_x^2)v(\cdot,t)\|_j \leq C\epsilon^2 t, \tag{3.11}$$

$$\|\eta(\cdot,t) - \tfrac{1}{2}(\alpha(\cdot,t)+\beta(\cdot,t))\|_j + \|v(\cdot,t) - \tfrac{1}{2}(1-\tfrac{\epsilon}{6}\partial_x^2)^{-1}(\alpha(\cdot,t)-\beta(\cdot,t))\|_j \leq C\epsilon^2 t, \tag{3.12}$$

and (in case $g(x) = h(x)$)

$$\|\eta(\cdot,t) - r(\cdot,t)\|_j + \|v(\cdot,t) - (1 - \tfrac{\epsilon}{6}\partial_x^2)^{-1}r(\cdot,t)\|_j \leq C\epsilon^2 t. \tag{3.13}$$

Proof. By Theorem 2.1, a solution (η, v) of (1.1) with the given initial data exists in $\mathcal{H}^J_{T_1} \times \mathcal{H}^J_{T_1}$ for some $T_1 > 0$. Now if J is sufficiently large, then by Corollary 3.2 of [11],

$$\|\eta - \eta_{app}\|_{j+2} + \|v - (1 - \tfrac{\epsilon}{6}\partial_x^2)^{-1}v_{app}\|_{j+2} \leq C\epsilon^2 t \tag{3.14}$$

for all $t \in [0, T_1]$, where (η_{app}, v_{app}) is as defined in (3.9) of [11]. (To correct a minor error in Corollary 3.2 of [11], one should replace the factor $(1 + \frac{\epsilon}{2}\eta_0)$ by $(1 - \frac{\epsilon}{2}\eta_0)^{-1}$. Note that this change does not affect the validity of the proof given there, since this same modification can be made in the statement and proof of Proposition 2.2 of [11].) Also, by Theorem 3.2 of [11]

$$\|\tilde{\eta} - \eta_{app}\|_j + \|\tilde{u} - v_{app}\|_j \leq C\epsilon^2 t \tag{3.15}$$

for all $t \in [0, T_1]$. Since $(1 - \frac{\epsilon}{6}\partial_x^2)$ is a bounded operator from H^{j+2} to H^j, it follows from (3.14) and (3.15) that

$$\|\tilde{\eta} - \eta\|_j + \|\tilde{u} - (1 - \frac{\epsilon}{6}\partial_x^2)v\|_j \leq C\epsilon^2 t$$

for all $t \in [0, T_1]$. Since this estimate establishes an L_2 bound on (v, η), it follows from Theorem 2.1 that T_1 can be taken equal to T. This completes the proof of (3.11). Estimates (3.12) and (3.13) then follow immediately from (3.8), (3.9), and the triangle inequality. □

Remark 3.9. It is straightforward to ascertain that an argument similar to that made in proving Theorem 3.5 shows that in the estimate (3.13), the function $(1-\frac{\epsilon}{6}\partial_x^2)^{-1}r(\cdot,t)$ can be replaced by $r_1(\cdot,t)$, where r_1 is defined as the solution of (1.5) with initial data $r_1(x,0)=(1-\frac{\epsilon}{6}\partial_x^2)^{-1}g(x)$. Similarly, in (3.6) the function $z(\cdot,t)$ can be replaced by $r_2(\cdot,t)$, where r_2 is defined as the solution of (1.5) with initial data $r_2(x,0)=g(x)-\frac{1}{4}\epsilon g(x)^2$. Thus (3.6) and (3.13) both provide comparison results between solutions (η,v) of (1.1) and pairs of solutions of the KdV equation (1.5). (The discrepancy between r_1 and r_2 is due, of course, to the fact that $h(x)=g(x)$ in (3.13) while $h(x)=g(x)-\frac{1}{4}\epsilon g(x)^2$ in (3.6).) An advantage of (3.13) is that the estimate is valid on a time scale of length D/ϵ, where D can be taken arbitrarily large (provided, of course, that ϵ is sufficiently small). On the other hand, (3.6) has the advantage of requiring a weaker assumption on the spatial decay of the initial data.

We now turn to the proof of Theorem 3.4, which will be accomplished in two stages. In Subsection 3.2, the proof of Theorem 3.4 is considered in the case $j=0$. The detailed analysis of this case points the way to the general case. Moreover, the general case, established in Subsection 3.3, is made by an induction argument wherein the result for $j=0$ is the starting point.

3.2. **Proof of Theorem 3.4 in the case $j=0$.** One easily verifies that r and z satisfy the equations

$$\begin{aligned} r_t+z_x+\epsilon(rz)_x-\tfrac{1}{6}\,\epsilon r_{xxt}&=-\epsilon^2G_1,\\ z_t+r_x+\epsilon zz_x-\tfrac{1}{6}\,\epsilon z_{xxt}&=-\epsilon^2G_2-\epsilon^3G_3, \end{aligned}$$

where $G_1=\frac{3}{4}\,r^2r_x-\frac{1}{4}(rr_x)_{xx}-\frac{1}{36}r_{xxxxx}$, $G_2=-\frac{1}{12}\,rr_{xxx}-\frac{1}{24}\,(r^2)_{xxt}$, $G_3=-\frac{1}{8}\,r^3r_x$.

Interest naturally focuses upon the differences $m=\eta-r$ and $n=v-z$ which satisfy the equations

$$\begin{aligned} m_t+n_x+\epsilon(mn)_x+\epsilon(rn)_x+\epsilon(zm)_x-\tfrac{1}{6}\,\epsilon m_{xxt}&=\epsilon^2G_1,\\ n_t+m_x+\epsilon(nn_x)+\epsilon(zn)_x-\tfrac{1}{6}\,\epsilon n_{xxt}&=\epsilon^2G_2+\epsilon^3G_3. \end{aligned} \tag{3.16}$$

and have initial values $m(x,0)\equiv n(x,0)\equiv 0$.

Multiply the first equation in (3.16) by m and the second by n, add the results, and then integrate over $\mathbb{R}\times[0,t]$. After suitable integrations by parts, there appears the formula

$$\frac{1}{2}\int_{-\infty}^{\infty}\Big[m^2+n^2+\frac{1}{6}\epsilon m_x^2+\frac{1}{6}\epsilon n_x^2\Big]\,dx \tag{3.17}$$

$$= -\epsilon \int_0^t \int_{-\infty}^{\infty} \left(m(mn)_x + m(rn)_x + m(zm)_x + n^2 n_x + n(zn)_x \right) \, dx \, d\tau$$
$$+ \epsilon^2 \int_0^t \int_{-\infty}^{\infty} (mG_1 + nG_2) \, dx \, d\tau + \epsilon^3 \int_0^t \int_{-\infty}^{\infty} nG_3 \, dx \, d\tau.$$

The idea is to derive from (3.17) a differential inequality that will imply the desired result via a Gronwall-type lemma. The argument put forward below for accomplishing this requires ϵ-independent bounds on r and its derivatives, as furnished by the following Lemma.

Lemma 3.10. *Let $s \geq 1$ be an integer. Then for every $K > 0$, there exists $C > 0$ such that the following is true. Suppose $g \in H^s$ with $\|g\|_s \leq K$, and let r be the solution of the KdV equation (1.5) with initial data $r(x,0) = g(x)$. Then for all $\epsilon \in (0,1]$ and all $t \geq 0$,*

$$\|r\|_s \leq C.$$

Also, for every integer k such that $1 \leq 3k \leq s$, one may further assert that

$$\|\partial_t^k r\|_{s-3k} \leq C.$$

This familiar result is a consequence of the existence of infinitely many conservation laws for KdV, together with the arguments put forward in [16]. Details are provided in the Appendix so this side issue does not distract from the main line of argument.

We remark that it follows immediately from Lemma 3.10 and (3.5) that r, z and their derivatives with respect to x up to order 5 are bounded in L_2 norm by constants which depend only on K, and which in particular are independent of t and ϵ. In what follows, we will use this fact without further comment, denoting all occurrences of such constants by C.

Define the quantity $A(t)$ to be the positive square root of the integral on the left-hand side of (3.17); *viz.*,

$$A^2(t) = \int_{-\infty}^{\infty} \left[m^2 + n^2 + \tfrac{1}{6}\epsilon m_x^2 + \tfrac{1}{6}\epsilon n_x^2 \right] dx.$$

From this definition it is obvious that for all t, we have

$$\|m\|_{L_2} \leq A(t) \quad \text{and} \quad \|m_x\|_{L_2} \leq C\epsilon^{-\frac{1}{2}} A(t).$$

Because of the elementary estimate

$$\|m\|_{L_\infty}^2 \leq \|m\|_{L_2} \|m_x\|_{L_2},$$

it then follows also that

$$\|m\|_{L_\infty} \leq C\epsilon^{-\frac{1}{4}} A(t).$$

Of course, the same estimates hold for n.

Now rewrite (3.17) as

$$\tfrac{1}{2}A^2(t) = I_1 + I_2 + I_3 + I_4, \tag{3.18}$$

where

$$\begin{aligned}
I_1 &= -\epsilon \int_0^t \int_{-\infty}^{\infty} m(mn)_x \; dx \; d\tau = \epsilon \int_0^t \int_{-\infty}^{\infty} nmm_x \; dx \; d\tau, \\
I_2 &= -\epsilon \int_0^t \int_{-\infty}^{\infty} m(rn)_x \; dx \; d\tau = \epsilon \int_0^t \int_{-\infty}^{\infty} rnm_x \; dx \; d\tau, \\
I_3 &= -\epsilon \int_0^t \int_{-\infty}^{\infty} [m(zm)_x + n(zn)_x] \; dx \; d\tau \\
&= -\frac{\epsilon}{2} \int_0^t \int_{-\infty}^{\infty} z_x(m^2 + n^2) \; dx \; d\tau, \\
I_4 &= \epsilon^2 \int_0^t \int_{-\infty}^{\infty} (mG_1 + nG_2) \; dx \; d\tau + \epsilon^3 \int_0^t \int_{-\infty}^{\infty} nG_3 \; dx \; d\tau.
\end{aligned}$$

Three of these quantities may be easily estimated as follows:

$$I_1 \leq \epsilon \int_0^t \|n\|_{L_\infty} \|m\|_{L_2} \|m_x\|_{L_2} \; d\tau \leq C\epsilon^{\frac{1}{4}} \int_0^t A^3(\tau) \; d\tau, \tag{3.19}$$

$$I_3 \leq C\epsilon \int_0^t A^2(\tau) d\tau,$$

and

$$I_4 \leq C\epsilon^2 \int_0^t A(\tau) \; d\tau + C\epsilon^3 \int_0^t A(\tau) \; d\tau.$$

It remains to estimate I_2. This apparently simple task is complicated by the requirement of not losing a factor of $\epsilon^{\frac{1}{2}}$, as this would lead to an inferior result to that stated in the theorem. Indeed, if one were to make the obvious estimate

$$I_2 \leq C\epsilon^{\frac{1}{2}} \int_0^t A^2(\tau) \; d\tau, \tag{3.20}$$

the best one could then do using Gronwall's inequality would be to establish a close comparison on a time interval of order $\epsilon^{-\frac{1}{2}}$, rather than on the desired interval of order ϵ^{-1}. Here instead of (3.20) we will use the considerably less straightforward estimate

$$I_2 \leq C\epsilon A^2(t) + C \int_0^t \left[\epsilon^3 A(\tau) + \epsilon A^2(\tau) + \epsilon^{\frac{5}{4}} A^3(\tau)\right] \; d\tau. \tag{3.21}$$

To prove (3.21), we begin by multiplying the second equation in (3.16) by rn and integrating over $\mathbb{R} \times [0,t]$ to obtain

$$\int_0^t \int_{-\infty}^{\infty} rnm_x \, dx \, d\tau = K_1 + K_2 + K_3 + K_4 + K_5,$$

where

$$K_1 = -\int_0^t \int_{-\infty}^{\infty} rnn_t \, dx \, d\tau, \qquad K_2 = -\epsilon \int_0^t \int_{-\infty}^{\infty} rn^2 n_x \, dx \, d\tau,$$
$$K_3 = -\epsilon \int_0^t \int_{-\infty}^{\infty} rn(zn)_x \, dx \, d\tau, \quad K_4 = \frac{1}{6} \, \epsilon \int_0^t \int_{-\infty}^{\infty} rnn_{xxt} \, dx \, d\tau,$$
$$K_5 = \epsilon^2 \int_0^t \int_{-\infty}^{\infty} (G_2 rn + \epsilon G_3 rn) \, dx \, d\tau.$$

To estimate K_1, integrate by parts with respect to t and use the fact that $n(x,0) \equiv 0$ to derive

$$K_1 = \frac{1}{2} \int_0^t \int_{-\infty}^{\infty} r_t n^2 \, dx \, d\tau - \frac{1}{2} \int_{-\infty}^{\infty} r(x,t) n^2(x,t) \, dx.$$

In consequence, one has that

$$|K_1| \leq C \int_0^t A^2(\tau) \, d\tau + CA^2(t). \tag{3.22}$$

For K_2, it transpires that

$$|K_2| \leq C\epsilon \int_0^t \|n\|_{L_\infty} \|n\|_{L_2} \|n_x\|_{L_2} \, d\tau \leq C\epsilon^{\frac{1}{4}} \int_0^t A^3(\tau) \, d\tau. \tag{3.23}$$

The third integral, K_3, may be rewritten as

$$K_3 = \frac{\epsilon}{2} \int_0^t \int_{-\infty}^{\infty} (r_x z - r z_x) n^2 \, dx \, d\tau,$$

whence one obtains

$$|K_3| \leq C\epsilon \int_0^t A^2(\tau) \, d\tau. \tag{3.24}$$

The estimate for K_5 is also straightforward, *viz.*,

$$|K_5| \leq C\epsilon^2 \int_0^t \|n\|_{L_2} \, d\tau \leq C\epsilon^2 \int_0^t A(\tau) \, d\tau. \tag{3.25}$$

The fourth integral K_4 is bounded by a more complicated argument. Start by writing

$$K_4 = -\frac{1}{6}\epsilon \int_0^t \int_{-\infty}^{\infty} (rn)_x n_{xt}\ dx\ d\tau$$
$$= -\frac{1}{6}\epsilon \int_0^t \int_{-\infty}^{\infty} r n_x n_{xt}\ dx\ d\tau - \frac{1}{6}\epsilon \int_0^t \int_{-\infty}^{\infty} r_x n n_{xt}\ dx\ d\tau = K_{41} + K_{42},$$

say. Using again the fact that n vanishes at $t = 0$, we have

$$K_{41} = -\frac{1}{6}\epsilon \int_0^t \int_{-\infty}^{\infty} \frac{1}{2} r (n_x^2)_t\ dx\ d\tau$$
$$= -\frac{1}{12}\epsilon \int_{-\infty}^{\infty} r(x,t) n_x^2(x,t)\ dx + \frac{1}{12}\epsilon \int_0^t \int_{-\infty}^{\infty} r_t n_x^2\ dx\ d\tau,$$

and it follows directly that

$$|K_{41}| \le CA^2(t) + C\int_0^t A^2(\tau)\ d\tau. \tag{3.26}$$

For K_{42}, integrate by parts in x to get

$$K_{42} = \frac{1}{6}\ \epsilon \int_0^t \int_{-\infty}^{\infty} r_{xx} n n_t\ dx\ d\tau + \frac{1}{6}\ \epsilon \int_0^t \int_{-\infty}^{\infty} r_x n_x n_t\ dx\ d\tau = K_{421} + K_{422}.$$

Now for K_{421}, integrate by parts with respect to t as for K_1 to reach the inequality

$$|K_{421}| \le C\epsilon^{\frac{3}{4}} A^2(t) + C\epsilon \int_0^t A^2(\tau)\ d\tau. \tag{3.27}$$

(In obtaining (3.27), one uses Lemma 3.10 to obtain a bound for $\|r_{xxt}\|$ which depends only on K.)

To obtain an effective bound on K_{422}, write the second equation in (3.16) in the form

$$n_t = \mathcal{K}_\epsilon * (m + \frac{\epsilon}{2} n^2 + \epsilon z n) - \mathcal{M}_\epsilon * (\epsilon^2 G_2 + \epsilon^3 G_3). \tag{3.28}$$

This formulation is obtained just as for the differential-integral equations (2.1) by first inverting $(1 - \frac{\epsilon}{6}\partial_x^2)$ and then integrating the terms involving $m_x, \epsilon n n_x$ and $\epsilon(zn)_x$ by parts. Using the form (3.28) for n_t in K_{422} and applying the elementary inequalities in Lemma 2.3 connected to convolution with $\mathcal{K}_\epsilon$ and $\mathcal{M}_\epsilon$, we derive that

$$|K_{422}| \le C\epsilon \int_0^t \|n_x\|_{L_2} \|n_t\|_{L_2}\ d\tau \tag{3.29}$$

$$\leq C\epsilon \int_0^t \|n_x\|_{L_2} \left[\epsilon^{-\frac{1}{2}}\|m + \frac{\epsilon}{2}n^2 + \epsilon zn\|_{L_2} + \epsilon^2\|G_2\|_{L_2} + \epsilon^3\|G_3\|_{L_2}\right]\, d\tau$$
$$\leq C\int_0^t \left[\epsilon^{\frac{5}{2}}A(\tau) + A^2(\tau) + \epsilon A^3(\tau)\right]\, d\tau.$$

Adding the inequalities (3.26), (3.27), and (3.29) leads to the bound

$$|K_4| \leq CA^2(t) + C\int_0^t \left[\epsilon^{\frac{5}{2}}A(\tau) + A^2(\tau) + \epsilon A^3(\tau)\right]\, d\tau. \tag{3.30}$$

Finally, putting together the estimates (3.22) for K_1, (3.23) for K_2, (3.24) for K_3, (3.25) for K_5, and (3.30) for K_4, there obtains the desired inequality (3.21).

Now combining (3.21) with the estimates for I_1, I_3 and I_4 obtained above, we deduce from (3.18) that for all positive ϵ small enough, say $\epsilon \in (0, \epsilon_1)$,

$$A^2(t) \leq C\int_0^t \left[\epsilon^2 A(\tau) + \epsilon A^2(\tau) + \epsilon^{\frac{1}{4}}A^3(\tau)\right]\, d\tau. \tag{3.31}$$

Of course, once ϵ_1 is fixed, then it is easy to prove that (3.31) holds as well (with a possibly larger value of C) for all $\epsilon \geq \epsilon_1$, since (3.20) implies that

$$I_2 \leq \frac{C}{\sqrt{\epsilon_1}}\, \epsilon \int_0^t A^2(\tau)\, d\tau$$

whenever $\epsilon \geq \epsilon_1$.

From (3.31) and Young's inequality, it follows that

$$A^2(t) \leq C\int_0^t [\epsilon^2 A(\tau) + A^3(\tau)]\, d\tau. \tag{3.32}$$

The following Gronwall-type lemma now comes to our aid. The proof is standard (see, e.g., [2], Lemma 2).

Lemma 3.11. *Let $\alpha > 0$, $\beta > 0$ and $\rho > 1$ be given. Define*

$$T = \beta^{-\frac{1}{\rho}}\alpha^{\frac{1-\rho}{\rho}} \int_0^\infty (1 + x^\rho)^{-1}\, dx.$$

Then there exists a constant $M = M(\rho) > 0$, which is independent of α and β, such that for any $T_1 \in [0, T]$, if $A(t)$ is a non-negative, continuous function defined on $[0, T_1]$ satisfying $A(0) = 0$ and

$$A^2(t) \leq \int_0^t [\alpha A(\tau) + \beta A^{\rho+1}(\tau)]\, d\tau$$

for all $t \in [0, T_1]$, then $A(t) \leq M\alpha t$ for all $t \in [0, T_1]$.

Applying Lemma 3.11 to (3.32) with $\alpha = C\epsilon^2$, $\beta = C$, and $\rho = 2$, we obtain that $A(t) \le C\epsilon^2 t$ for all $t \in [0, D\epsilon^{-1}]$, where D, like C, is a constant depending only on K. This in turn implies that

$$\|\eta(\cdot,t) - r(\cdot,t)\|_{L_2} + \|v(\cdot,t) - z(\cdot,t)\|_{L_2} \le C\epsilon^2 t, \tag{3.33}$$

at least for $0 \le t \le D\epsilon^{-1}$, which is the advertised result when $j = 0$.

The preceding inequalities were all predicated on the existence of the solution pair (η, v) of the Boussinesq system with initial data as in (3.1) based on g. The local existence theory in Section 2 guarantees that there is such a solution at least over some positive time interval. Moreover, as long as the L_2 norms $\|\eta(\cdot,t)\|_{L_2}$ and $\|v(\cdot,t)\|_{L_2}$ remain bounded, the solution continues to persist at whatever level of regularity is afforded by the initial data, according to Theorem 2.1.

Suppose now that $g \in H^5$. According to the above calculations, it is known that (3.33) holds at least for $0 \le t < T = \min(T_0, D/\epsilon)$, where T_0 is the maximum existence time for the solution (η, v) of (1.1) with initial data as in (3.1). On the other hand, as long as (3.33) holds, the triangle inequality implies that

$$\|\eta\|_{L_2} \le \|\eta - r\|_{L_2} + \|r\|_{L_2}, \qquad \|v\|_{L_2} \le \|v - z\|_{L_2} + \|z\|_{L_2}.$$

Thus Lemma 3.3 and (3.33) combine to yield L_2 bounds on η and v. This in turn implies that $T_0 \ge D/\epsilon$. The proof of Theorem 3.4 in the case $j = 0$ is now complete.

3.3. **Proof of Theorem 3.1 in the case $j \ge 1$.** In this subsection, consideration is given to comparison of (r, z) and (η, v) in the Sobolev spaces H^j, $j \ge 1$. The argument is made by induction on j, the case $j = 0$ being in hand.

Define the quantity $A_j(t)$ to be the natural generalization of the function A that appeared in Subsection 3.1, namely, the positive square root of

$$A_j^2(t) = \int_{-\infty}^{\infty} \sum_{k=0}^{j} \left[m_{(k)}^2 + n_{(k)}^2 + \frac{1}{6}\epsilon m_{(k+1)}^2 + \frac{1}{6}\epsilon n_{(k+1)}^2 \right] dx,$$

where for any integer $l \ge 0$, $m_{(l)}$ denotes $\frac{\partial^l m}{\partial x^l}$ and similarly for $n_{(l)}$. The aim is to prove that there exist C_j and D_j such that if $t \in [0, D_j\epsilon^{-1}]$, then

$$A_j(t) \le C_j\epsilon^2 t.$$

In the previous subsection, this was proved to be true for $j = 0$. Fix $j \ge 1$ and assume the result has been proved for $j - 1$. We attempt to show that it holds for j.

Taking the j^{th} derivative of equations (3.16) with respect to x yields

$$\begin{aligned}&\partial_t m_{(j)} + n_{(j+1)} + \epsilon(mn)_{(j+1)} \\ &+ \epsilon(rn)_{(j+1)} + \epsilon(zm)_{(j+1)} - \frac{1}{6}\epsilon\partial_t m_{(j+2)} = \epsilon^2(G_1)_{(j)}\end{aligned} \tag{3.34}$$

and

$$\begin{aligned}&\partial_t n_{(j)} + m_{(j+1)} + \epsilon(nn_x)_{(j)} \\ &+ \epsilon(zn)_{(j+1)} - \frac{1}{6}\epsilon\partial_t n_{(j+2)} = \epsilon^2(G_2)_{(j)} + \epsilon^3(G_3)_{(j)}.\end{aligned} \tag{3.35}$$

(Note that according to Theorem 2.1, η and v, and hence also m and n, exist and remain in H^{j+5} at least for $t \in [0, D_{j-1}\epsilon^{-1}]$, so the manipulations here are justified.) Multiply (3.34) by $m_{(j)}$ and (3.35) by $n_{(j)}$, add the results, and integrate over $\mathbb{R} \times [0,t]$ to reach the relation

$$\frac{1}{2}\int_{-\infty}^{\infty}\left[m_{(j)}^2 + n_{(j)}^2 + \frac{1}{6}\epsilon\, m_{(j+1)}^2 + \frac{1}{6}\epsilon\, n_{(j+1)}^2\right] dx = I_1 + I_2 + I_3 + I_4,$$

where

$$\begin{aligned}I_1 &= -\epsilon\int_0^t\int_{-\infty}^{\infty}\left[(mn)_{(j+1)}m_{(j)} + (nn_x)_{(j)}n_{(j)}\right]\, dx\, d\tau,\\ I_2 &= -\epsilon\int_0^t\int_{-\infty}^{\infty}(rn)_{(j+1)}m_{(j)}\, dx\, d\tau,\\ I_3 &= -\epsilon\int_0^t\int_{-\infty}^{\infty}\left[(zm)_{(j+1)}m_{(j)} + (zn)_{(j+1)}n_{(j)}\right]\, dx\, d\tau,\\ I_4 &= \epsilon^2\int_0^t\int_{-\infty}^{\infty}\left[(G_1)_{(j)}m_{(j)} + (G_2)_{(j)}n_{(j)}\right]\, dx\, d\tau\\ &\quad + \epsilon^3\int_0^t\int_{-\infty}^{\infty}(G_3)_{(j)}n_{(j)}\, dx\, d\tau.\end{aligned}$$

Our aim is to obtain estimates for I_1 through I_4 in terms of constants which depend only on $\|g\|_{j+5}$, and hence only on K. (In what follows, we continue to denote all such constants by C.) Because of the induction hypothesis, it is known that there exist constants $C_{j-1} > 0$ and $D_{j-1} > 0$, depending only on $\|g\|_{j+4}$, such that

$$\|m\|_{j-1} + \|n\|_{j-1} = \|\eta - r\|_{j-1} + \|v - z\|_{j-1} \le C_{j-1}\epsilon^2 t$$

holds for all $t \in [0, D_{j-1}\epsilon^{-1}]$. In particular,

$$\|m\|_{j-1} + \|n\|_{j-1} \le C_{j-1}D_{j-1}\epsilon$$

for all $t \in [0, D_{j-1}\epsilon^{-1}]$. It follows immediately that $\|m\|_{j-1} \leq C$ and $\|n\|_{j-1} \leq C$. These estimates will be used repeatedly in the induction step.

The integrand in I_1 can be expanded into a sum of terms of the form $m_{(k)}m_{(i)}n_{(l)}$ and $n_{(k)}n_{(i)}n_{(l)}$, in which each of k, i, and l is less than or equal to $j+1$, but no two can both equal $j+1$ in any term. Therefore, arguing as in establishing (3.19), it is concluded that

$$|I_1| \leq C\epsilon^{\frac{1}{4}} \int_0^t A_j^3(\tau)\ d\tau. \tag{3.36}$$

To estimate I_4, use Hölder's inequality to obtain

$$|I_4| \leq C\epsilon^2 \int_0^t A_j(\tau)\ d\tau.$$

The term I_3 can be analyzed by writing

$$\begin{aligned} I_3 =& -\epsilon \int_0^t \int_{-\infty}^{\infty} \Big[z(m_{(j+1)}m_{(j)} + n_{(j+1)}n_{(j)}) \\ &+ \sum_{k=1}^{j+1} \binom{j+1}{k} z_{(k)}(m_{(j+1-k)}m_{(j)} + n_{(j+1-k)}n_{(j)}) \Big]\ dx\ d\tau \\ =& \frac{1}{2}\ \epsilon \int_0^t \int_{-\infty}^{\infty} (m_{(j)}^2 + n_{(j)}^2) z_x\ dx\ d\tau \\ &- \epsilon \int_0^t \int_{-\infty}^{\infty} \sum_{k=1}^{j+1} \binom{j+1}{k} z_{(k)}(m_{(j+1-k)}m_{(j)} + n_{(j+1-k)}n_{(j)})\ dx\ d\tau, \end{aligned}$$

from which it is obvious that

$$|I_3| \leq C\epsilon \int_0^t A_j^2(\tau)\ d\tau.$$

It remains to estimate I_2. Multiplying equation (3.35) by $rn_{(j)}$ and integrating over $\mathbb{R} \times [0,t]$, it transpires that

$$\int_0^t \int_{-\infty}^{\infty} rn_{(j)}m_{(j+1)}\ dx\ d\tau = K_1 + K_2 + K_3 + K_4 + K_5, \tag{3.37}$$

where

$$K_1 = -\int_0^t \int_{-\infty}^{\infty} r n_{(j)} \partial_t n_{(j)} \, dx \, d\tau,$$
$$K_2 = -\epsilon \int_0^t \int_{-\infty}^{\infty} r n_{(j)} (n n_x)_{(j)} \, dx \, d\tau,$$
$$K_3 = -\epsilon \int_0^t \int_{-\infty}^{\infty} r n_{(j)} (z n)_{(j+1)} \, dx \, d\tau,$$
$$K_4 = \frac{1}{6} \, \epsilon \int_0^t \int_{-\infty}^{\infty} r n_{(j)} \partial_t n_{(j+2)} \, dx \, d\tau,$$
$$K_5 = \epsilon^2 \int_0^t \int_{-\infty}^{\infty} r n_{(j)} \left((G_2)_{(j)} + \epsilon (G_3)_{(j)} \right) \, dx \, d\tau.$$

The integral I_2 may be written as

$$I_2 = \epsilon \int_0^t \int_{-\infty}^{\infty} (rn)_{(j)} m_{(j+1)} \, dx \, d\tau = \epsilon \int_0^t \int_{-\infty}^{\infty} r n_{(j)} m_{(j+1)} \, dx \, d\tau$$
$$+ \epsilon \int_0^t \int_{-\infty}^{\infty} \sum_{k=1}^{j} \binom{j}{k} r_{(k)} n_{(j-k)} m_{(j+1)} \, dx \, d\tau,$$

and the last term on the right-hand side is easily seen to be bounded by

$$C\epsilon \int_0^t A_j^2(\tau) \, d\tau,$$

so the key to understanding I_2 is to obtain a bound for the integral in (3.37).

We begin estimating the summands K_1 through K_5 in (3.37). First, note that the same argument used to obtain (3.22) gives here

$$|K_1| \le C A_j^2(t) + C \int_0^t A_j^2(\tau) \, d\tau,$$

and the same argument used to obtain (3.36) gives

$$|K_2| \le C\epsilon^{\frac{1}{2}} \int_0^t A_j^3(\tau) \, d\tau.$$

Similarly, obvious estimates yield

$$|K_3| \le C\epsilon^{\frac{1}{2}} \int_0^t A_j^2(\tau) \, d\tau \quad \text{and} \quad |K_5| \le C\epsilon^2 \int_0^t A_j(\tau) \, d\tau.$$

Attention is now turned to K_4. Integrating by parts leads to

$$K_4 = -\frac{1}{6}\,\epsilon \int_0^t \int_{-\infty}^{\infty} \left[r n_{(j+1)} \partial_t n_{(j+1)} + r_x n_{(j)} \partial_t n_{(j+1)} \right]\, dx\, d\tau = K_{41} + K_{42}.$$

The integral K_{41} can be handled in the same way as K_1, to reach the estimate

$$|K_{41}| \leq C A_j^2(t) + C \int_0^t A_j^2(\tau)\, d\tau.$$

The quantity K_{42} may also be handled in a way that is by now familiar: write

$$K_{42} = \frac{1}{6}\epsilon \int_0^t \int_{-\infty}^{\infty} \left[r_{xx} n_{(j)} \partial_t n_{(j)} + r_x n_{(j+1)} \partial_t n_{(j)} \right]\, dx\, d\tau = K_{421} + K_{422},$$

and follow the same procedure presented earlier for obtaining the estimates (3.27) and (3.29), using (3.35) to replace the term $\partial_t n_{(j)}$ in K_{422}. As a result, there obtains the estimate

$$|K_4| \leq C A_j^2(t) + C \int_0^t \left[\epsilon^{\frac{5}{2}} A_j(\tau) + A_j^2(\tau) + \epsilon A_j^3 \tau \right]\, d\tau,$$

as in (3.30).

Combining the inequalities for K_1 through K_5 implies

$$|K| \leq C A_j^2(t) + C \int_0^t \left[\epsilon^2 A_j(\tau) + A_j^2(\tau) + \epsilon^{\frac{1}{4}} A_j^3(\tau) \right]\, d\tau,$$

from which it follows that

$$|I_2| \leq C\epsilon A_j^2(t) + C \int_0^t \left[\epsilon^3 A_j(\tau) + \epsilon A_j^2(\tau) + \epsilon^{\frac{5}{4}} A_j^3(\tau) \right]\, d\tau.$$

Finally, putting together the estimates for I_1 through I_4, the analogue of (3.31) appears, namely

$$A_j^2(t) \leq C \int_0^t \left[\epsilon^2 A_j(\tau) + \epsilon A_j^2(\tau) + \epsilon^{\frac{1}{4}} A_j^3(\tau) \right]\, d\tau.$$

This inequality, valid for $0 \leq t \leq D_{j-1}\epsilon^{-1}$, taken together with Lemma 3.11, allows the conclusion that there are constants C_j and D_j depending only on $\|g\|_{j+5}$ such that

$$A_j(t) \leq C_j \epsilon^2 t \quad \text{for} \quad 0 \leq t \leq D_j \epsilon^{-1}.$$

Thus, the proof of Theorem 3.4 is complete.

4. Numerical Results

The theoretical results established in Section 3 are augmented by a numerical study reported in the present section. There are several issues of both theoretical and practical importance that are especially illuminated by numerical simulations. First, one would like an idea of how large are the various constants that depend upon norms of the initial data $\|g\|$. They are independent of ϵ for $\epsilon \in (0, 1]$, but if, for example, the constant C in Theorem 3.1 is some enormous multiple of the norm of the initial data or the constant D is a very small number, then the result has correspondingly less value. Next, it is to be expected that if only small values of ϵ are considered, then the values of the constants can be improved, and presumably take on an asymptotic best value as ϵ approaches zero. An important question then is to understand just how small must ϵ be in order for the constants to approximate well their asymptotic values. A related question is whether the comparison estimate (3.4) is sharp in the sense that ϵ^2 is the highest power of ϵ that can appear there. Finally, one might ask whether the time interval of comparison in (3.3) can be extended to a longer interval, such as $[0, \epsilon^{-2}]$. Since our analytical approach casts little light on these detailed points, we have resorted to a series of numerical experiments designed to elucidate the issues.

The numerical algorithm used is based on the integral equation formulation (2.2) of (1.1) and a similar formulation of (1.4) (see [3]). The details of the numerical procedure are presented in [8] for (1.1) and [15] for (1.4). While there is no reason to report the details again here, it is worth remarking that these numerical schemes are proved to be fourth-order accurate in space and in time, to be unconditionally stable, and to have the optimal order of efficiency, namely the number of operations required for each time step is $O(N)$, where N is the number of spatial mesh points.

In the present implementation of the algorithms, the solutions are approximated numerically on the spatial domain $0 \le x \le L$ with uniform mesh size, taken to be $\Delta x = \frac{1}{64}\sqrt{\epsilon}$. The spatial mesh points are thus given by $x_i = i\Delta x$ for $i = 0, 1, 2, \ldots, N$, where $N = \frac{L}{\Delta x}$. The time step Δt is taken equal to Δx. (Making Δx and Δt proportional to $\sqrt{\epsilon}$ renders them independent of ϵ in the original physical variables.) The length L of the spatial domain is chosen to be large enough that, for initial data representing a disturbance located far enough from the endpoints $x = 0$ and $x = L$, the boundary data at the endpoints (or, in the case of Experiment 4 below, at the right endpoint) can be safely taken equal to zero on the time interval under consideration. Typically, $L = 360\sqrt{\epsilon}$.

We now present and discuss the results of the numerical experiments. The first experiment, concerned with solitary waves, serves as a test of our coding in addition to continuing the conversation about the relation between (1.1) and (1.4).

Experiment 1: Solitary waves. In this experiment, an exact travelling-wave solution to (1.4) is compared with the corresponding solution of the initial-value problem for (1.1) as in Theorem 3.1. The initial data for (1.4) is taken to be

$$q_\epsilon(x,0) \equiv g_\epsilon(x) = \operatorname{sech}^2\Big(\tfrac{1}{2}\sqrt{\tfrac{3}{1+\epsilon/2}}(x-x_0)\Big).$$

The solution of the BBM equation corresponding to this initial data is the exact travelling wave solution $q_\epsilon(x,t) = g_\epsilon(x-kt)$, where $k = 1+\epsilon/2$ is the phase speed. Following (3.1), we seek a solution $(\eta_\epsilon, v_\epsilon)$ of (1.1) with initial data $\eta_\epsilon(x,0) = g_\epsilon(x)$ and $v_\epsilon(x,0) = g_\epsilon(x) - \frac{1}{4}\epsilon g_\epsilon(x)^2$.

An example of the results is shown in Figure 1(a), where the surface profile $\eta_\epsilon(x,t)$ is plotted with $\epsilon = 0.4$ and $x_0 = 19$. The solution is very nearly a travelling wave, like the solution $q_\epsilon(x,t)$ of (1.4), as was to be expected from the comparison result. It does have, however, a small dispersive tail.

According to Theorem 3.1, the solution $(\eta_\epsilon, v_\epsilon)$ should closely resemble (q_ϵ, w_ϵ), where $w_\epsilon(x,t) = q_\epsilon(x,t) - \frac{1}{4}\epsilon q_\epsilon(x,t)^2$. For purposes of comparison, the quantities

$$E_p(\epsilon,t) = \frac{|\eta_\epsilon(\cdot,t) - q_\epsilon(\cdot,t)|_p}{|q_\epsilon(\cdot,t)|_p} \quad \text{and} \quad \tilde{E}_p(\epsilon,t) = \frac{|v_\epsilon(\cdot,t) - w_\epsilon(\cdot,t)|_p}{|w_\epsilon(\cdot,t)|_p}$$

were computed, where $|\cdot|_p$ denotes a discrete approximation to the L_p norm on $[0,L]$. More precisely, for $1 \le p < \infty$, $|f|_p$ denotes the approximation to $\big(\int_0^L |f|^p\,dx\big)^{1/p}$ obtained by using Simpson's rule with grid points $\{x_i\}$, and for $p = \infty$, $|f|_p$ is defined by $|f|_\infty = \sup_i |f(x_i)|$. In Figure 1(b), E_p and $\tilde{E}_p$ are plotted against time t for $p = 2$ and $p = \infty$, over the interval $0 \le t \le 50$, again with $\epsilon = 0.4$. The top two curves, drawn with dashed lines, are the plots of E_2 and $\tilde{E}_2$; the plots of E_∞ and $\tilde{E}_\infty$ are drawn with solid lines, and appear to be one curve because they are almost identical. Figure 1(b) not only verifies that the relative differences increase linearly with time t for $t < C\epsilon^{-1}$, as asserted in Theorem 3.1 and Corollary 3.2, but also demonstrates that this linear estimate is valid for larger values of t. Similar results are found in Experiments 2–4 below, indicating that the time interval appearing in (3.3) is probably not the longest possible.

The solution profiles of (1.1) and (1.4) at $t = 50$ corresponding to the initial data described above (with $\epsilon = 0.4$ and $x_0 = 19$) are plotted in Figure

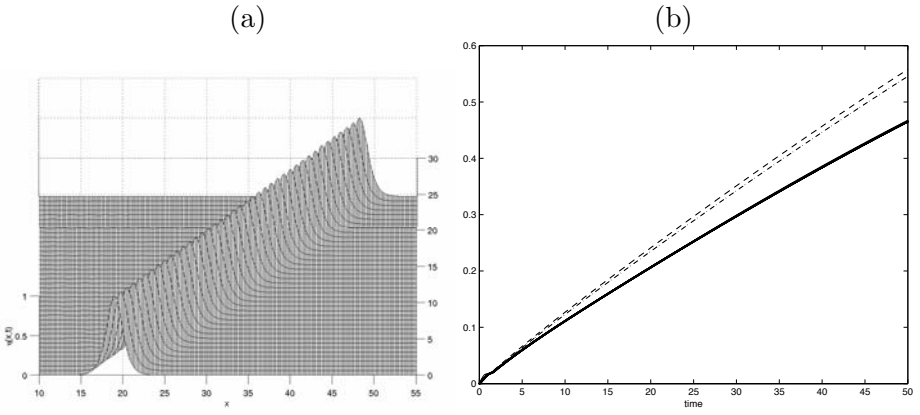

FIGURE 1. (a) Surface profile $\eta_\epsilon(x,t)$. (b) Relative differences between solutions of (1.1) and (1.4).

2(a), which shows that $\eta_\epsilon(x,50)$ and $q_\epsilon(x,50)$ have a very similar shape. However, as one sees upon consulting Figure 1(b), the relative difference between them, as measured by E_∞, is almost 0.5. This is clearly due to phase difference: the two equations propagate their respective travelling waves at noticeably different speeds. It is worth noting that this difference in the speed of propagation owes to nonlinear effects. Indeed, an eassy calculation shows that the linear forms of (1.1) and (1.4) (i.e., drop the quadratic terms) have exactly the same dispersion relation between frequency ω and wave number k, namely, $\omega(k) = k/(1+\frac{1}{6}\epsilon k^2)$ for waves moving to the right.

This leads one to imagine a comparison between solutions modulo a phase shift, or what is often called the shape difference [15]. For a fixed t, the phase shift is determined by first finding the mesh point x_k where $\eta_\epsilon(x_k,t)$ takes its maximum value, and then using a quadratic polynomial interpolating $(x_k,\eta_\epsilon(x_k,t))$ and the two neighboring points $(x_{k-1},\eta_\epsilon(x_{k-1},t))$ and $(x_{k+1},\eta_\epsilon(x_{k+1},t))$ to determine the location of the maximum point of $\eta_\epsilon(x,t)$; *viz.*,

$$x^* = \frac{(2x_k-\Delta x)\eta_\epsilon(x_{k+1},t) - 4x_k\eta_\epsilon(x_k,t) + (2x_k+\Delta x)\eta_\epsilon(x_{k-1},t)}{2\eta_\epsilon(x_{k+1},t) - 4\eta_\epsilon(x_k,t) - 2\eta_\epsilon(x_{k-1},t)}.$$

We then define $\eta^s_\epsilon(x,t) = \eta_\epsilon(x+x^*-x_0,t)$, and compute the "relative shape difference"

$$E^s_p(\epsilon,t) = \frac{|\eta^s_\epsilon(\cdot,t) - g_\epsilon(x)|_p}{|g_\epsilon(x)|_p}$$

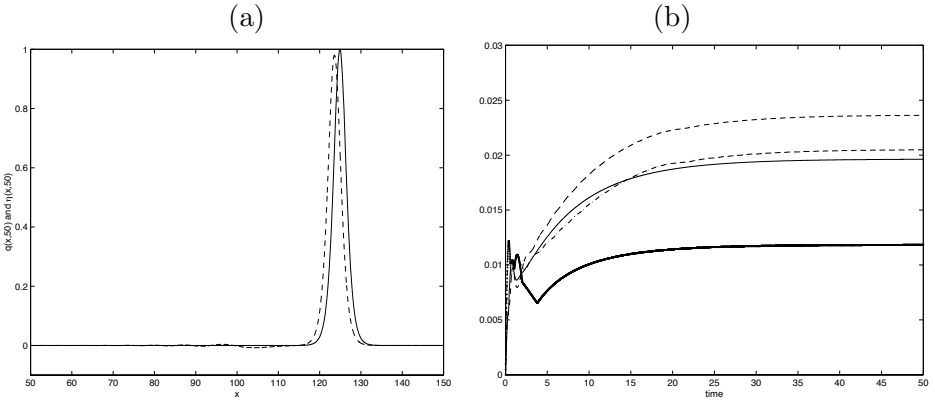

FIGURE 2. (a) A solution of (1.4) (solid line) and a corresponding solution of (1.1) (dashed line) at $t = 50$. (b) Relative shape differences between solutions of (1.4) and (1.1).

for $p = 2$ and $p = \infty$. Similarly, one can compute the relative difference

$$\tilde{E}_p^s(\epsilon, t) = \frac{|v_\epsilon^s(\cdot, t) - v_\epsilon(\cdot, 0)|_p}{|v_\epsilon(\cdot, 0)|_p}$$

between a shifted profile $v^s(x, t)$ and the initial data $v_\epsilon(x, 0)$. The results for $\epsilon = 0.4$ are shown in Figure 2(b), where the dotted curves represent E_2^s and $\tilde{E}_2^s$, and the solid curves represent E_∞^s and $\tilde{E}_\infty^s$. The relative shape differences remain less than 0.025 for t up to 50.

Results of this experiment for other values of ϵ are summarized in Tables 1 and 2. To maintain the accuracy, different values of x_0 were used so that the solution at the boundary would be consistently small over the entire temporal interval. The values of E_∞, $\tilde{E}_\infty$, E_2, and $\tilde{E}_2$ at $t = 50$ are listed in Table 1 for ϵ ranging from 0.025 to 0.6. The corresponding data on shape differences are listed in Table 2.

From rows 4–7 in Tables 1 and 2, one notices that the comparisons made via the discrete L_∞ or L_2 norms behave similarly. For either choice of norm, the relative error decreases as ϵ decreases, and the rates of decrease are comparable. For the rest of the discussion, therefore, we use as benchmarks the quantities $E_2(\epsilon, t)$ and $E_2^s(\epsilon, t)$.

Note that E_2 is decreasing as ϵ decreases (see row 6 in Table 1). The rate of decrease, computed by using the formula

$$\text{rate}(\epsilon_n) = \frac{\log\big(E_2(\epsilon_n, t)/E_2(\epsilon_{n+1}, t)\big)}{\log(\epsilon_n/\epsilon_{n+1})},$$

n	1	2	3	4	5	6	7	8
ϵ_n	0.6	0.5	0.4	0.3	0.2	0.1	0.05	0.025
x_0	20	20	19	17	14	12	9	9
E_∞	0.79	0.64	0.47	0.29	0.14	0.041	0.012	0.0032
$\tilde{E}_\infty$	0.79	0.64	0.47	0.29	0.14	0.041	0.012	0.0032
E_2	0.98	0.78	0.56	0.34	0.17	0.046	0.0013	0.0034
$\tilde{E}_2$	0.97	0.76	0.55	0.34	0.16	0.046	0.0013	0.0033
rate of E_2	1.3	1.5	1.7	1.8	1.8	1.9	1.9	$\to 2$

TABLE 1. The relative difference between solutions $(\eta_\epsilon, v_\epsilon)$ of (1.1) and (q_ϵ, w_ϵ) of (1.4) at $t = 50$, and the rate of decrease of E_2 with respect to ϵ.

n	1	2	3	4	5	6	7	8
ϵ_n	0.6	0.5	0.4	0.3	0.2	0.1	0.05	0.025
x_0	20	20	19	17	14	12	9	9
E^s_∞	0.031	0.025	0.020	0.014	0.0092	0.0040	0.0017	0.00067
$\tilde{E}^s_\infty$	0.0015	0.0014	0.0012	0.0097	0.0071	0.0037	0.0017	0.00066
E^s_2	0.0033	0.0028	0.0024	0.0019	0.0013	0.0061	0.0024	0.00085
$\tilde{E}^2_s$	0.027	0.024	0.020	0.017	0.012	0.0058	0.0023	0.00084
rate of E^s_2	0.83	0.82	0.83	0.90	1.1	1.3	1.5	

TABLE 2. The relative difference between solutions (q_ϵ, w_ϵ) of (1.4) and $(\eta^s_\epsilon(x,t), v^s_\epsilon(x,t))$, which are the shifts of solutions $(\eta_\epsilon, v_\epsilon)$ of (1.1), at $t = 50$, and the rate of decrease of E^s_2 with respect to ϵ.

is shown in row 8 of Table 1. The rate of decrease is also calculated for the shape difference (see row 8 of Table 2). For relatively small ϵ, the overall difference is decreasing quadratically. The shape difference is decreasing linearly with respect to ϵ for moderate ϵ. Using Richardson extrapolation on data at $\epsilon = 0.4$, 0.2, 0.1, 0.05 and 0.025, one finds that

$$E_2(\epsilon, 50) \approx 5.8\ \epsilon^2$$

as $\epsilon \to 0$. Therefore, the constant D_2 in Theorem 3.1 for $j = 0$ seems to be small (about 0.12 in this example).

Comparing the data in Table 1 and Table 2, one finds that the shape difference $E^s_2(\epsilon, t)$ is much smaller than the difference $E_2(\epsilon, t)$, especially for waves of moderate size. Using a least squares approximation on data listed

in row 6 of Table 2 at $\epsilon = 0.6, 0.5, \ldots, 0.025$, one obtains

$$E_2^s(\epsilon, 50) \approx 0.0494\ \epsilon.$$

From earlier studies (for example [13, 22]), it is known that the solitary-wave solutions of the BBM equation play the same sort of distinguished role in the long-time asymptotics of general disturbances that they do for the Korteweg-de Vries equation. The numerical simulations in [8] show that a similar conclusion is warranted for (1.1) (and see also [25]). Consequently, it is potentially telling that an individual solitary-wave solution of (1.4) is seen to be very close (with $E_2^s \leq 0.04$ for all amplitudes we have tried) to the solution of (1.1) when the one-way velocity assumption (3.1) is imposed. Moreover, the structure of the solution of (1.1), when initiated with the BBM solitary wave using (3.1), appears to be a solitary-wave solution of (1.1) followed by a very small dispersive tail. Thus, the impact of the present experiment could be much broader than appears at first sight.

Experiment 2: Waves with dispersive trains. In the first experiment, the initial profile g was chosen so that it generated an exact solution of the BBM equation. However, this initial data had to depend on ϵ, albeit weakly. In the next experiment, the initial data g is fixed, independently of ϵ. We choose for this case a g that results in a lot of dispersion: namely, a profile of the form

$$g(x) = \Big(-2 + \cosh\Big(3\sqrt{\tfrac{2}{5}}(x - x_0)\Big)\Big)\operatorname{sech}^4\Big(\tfrac{3(x-x_0)}{\sqrt{10}}\Big), \tag{4.1}$$

with two small crests separated by a deep trough. This profile, with $x_0 = 60$, is displayed as the top curve in Figure 3. The initial data for (1.1) is, as before, given by $\eta_\epsilon(x, 0) = g(x)$ and $v_\epsilon(x, 0) = g(x) - \frac{1}{4}\epsilon g^2(x)$. Figure 3 shows the solution profile $\eta_\epsilon(x, t)$ at $t = 0, 10, 20, 30$ and 40 with $\epsilon = 0.5$. It is clear that the wave propagates to the right and also expands slowly to the left, and decays in L_∞ norm, leaving a considerable dispersive tail behind. The solution profile $q_\epsilon(x, t)$ of (1.4) disperses similarly (see Figure 4).

Graphs of $\eta_\epsilon(x, t)$ and $q_\epsilon(x, t)$ at $t = 4.95$, 25.5, 49.5 are shown in Figure 4. It is clear that the two solutions are very close to each other. The relative differences E_2 and $\tilde{E}_2$ are plotted in Figure 5 for $\epsilon = 0.5$ and t between 0 and 50. The values of E_2 and $\tilde{E}_2$ increase relatively rapidly, but linearly, to about 0.1 by $t = 3$, and then more slowly thereafter. These numerical results are not only consistent with the theoretical result $|\eta_\epsilon - q_\epsilon|_{L_\infty} \leq C\epsilon^2 t$ for $t \leq D\epsilon^{-1}$, but also indicate that the result may well continue to larger values of t.

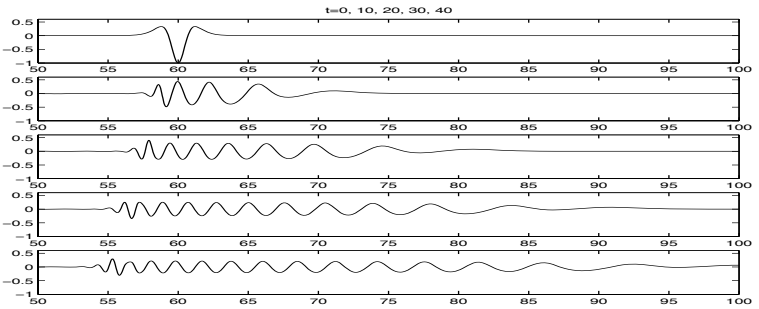

FIGURE 3. Solution of Boussinesq system with $\epsilon = 0.5$.

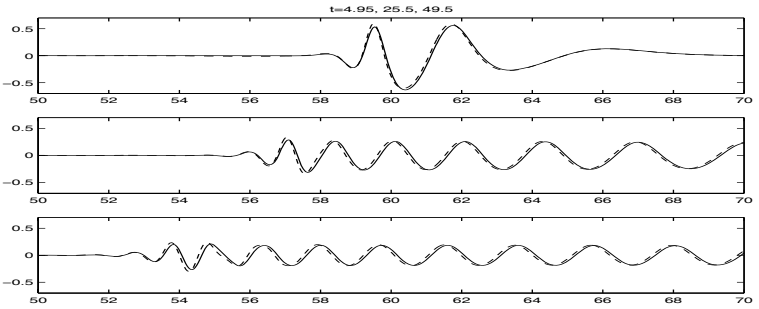

FIGURE 4. Comparison between solutions of BBM equation (solid line) and Boussinesq system (dashed line) with $\epsilon = 0.5$.

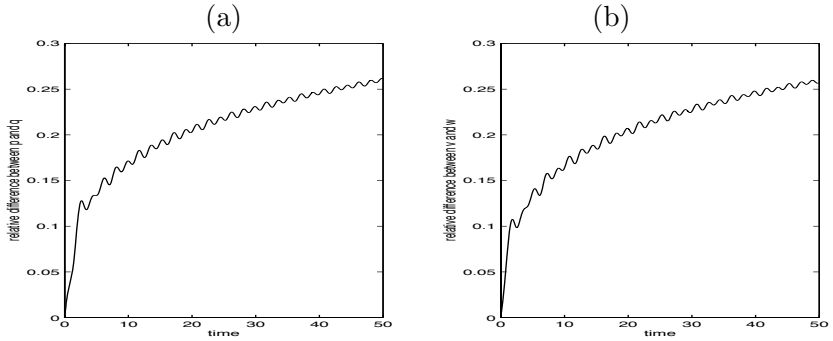

FIGURE 5. Comparison between solutions of BBM equation and Boussinesq system with $\epsilon = 0.5$, where (a) plots $E_2(\epsilon, t)$ and (b) plots $\tilde{E}_2(\epsilon, t)$.

ϵ	0.8	0.7	0.6	0.5	0.4	0.3	0.2	0.1	0.05
E_2	0.728	0.547	0.392	0.262	0.162	0.09.4	0.0525	0.0210	0.0090
rate on E_2	2.1	2.2	2.2	2.1	1.8	1.5	1.3	1.2	
D_2^s	0.476	0.307	0.180	0.0943	0.0561	0.00400	0.00263	0.00126	0.0061
rate on D_2^s	3.3	3.5	3.5	2.3	1.2	1.0	1.1	1.1	

TABLE 3. The relative difference and shape difference between solutions $(\eta_\epsilon, v_\epsilon)$ of (1.1) and (q_ϵ, w_ϵ) of (1.4) at $t = 50$, with initial data (4.1) for BBM.

One sees clearly from Figure 4 that η_ϵ and q_ϵ have a very similar shape for all values of t shown, but that there are small but persistent phase shifts between η_ϵ and q_ϵ that could lead to a large value of $E_2(\epsilon, t)$ (in fact $E_2(\epsilon, t)$ is about 0.26 when $t = 50$). Data on the relative difference $E_2(\epsilon, t)$ and relative shape difference $D_2^s(\epsilon, t)$ between η_ϵ and q_ϵ are listed in Tables 3 and 4. Here, because no exact solution is available for q_ϵ, the shape difference is calculated using a different approach than in Experiment 1. For $\alpha \in \mathbb{R}$ and t fixed, define $J(\alpha)$ by

$$J(\alpha) = \left\{ \int_0^L |\bar{\eta}_\epsilon(x,t) - \bar{q}_\epsilon(x-\alpha,t)|^2 \, dx \right\}^{\frac{1}{2}}$$

where $\bar{\eta}_\epsilon(x,t)$ and $\bar{q}_\epsilon(x,t)$ are the cubic spline interpolation functions through the points $\eta(x_i,t)$ and $q(x_i,t)$. The shape difference $D_2^s(\epsilon,t)$ is obtained by finding the minimum value of $J(\alpha)$. The Matlab program *fminbnd* is used in our computation.

Table 3 shows the dependence of $E_2(\epsilon,t)$ and $D_2^s(\epsilon,t)$ on ϵ for $t = 50$. The rate of convergence to 0 degrades as ϵ becomes smaller. Since this behavior does not match the expected asymptotic behavior as $\epsilon \to 0$, we investigated further using values of ϵ below 0.05. The results are shown in Table 4, where one eventually sees what looks like quadratic convergence in ϵ. These calculations were done at $t = 1$ since the t-dependence of E_2 for larger values of t is shown in Figure 5 already.

In general, for moderate sized waves, corresponding to say $\epsilon \leq 0.4$, the shape difference is small until t gets large. But for large ϵ and t, the shape difference can be large. (This is in contrast to the situation in Experiment 1, where the shape difference remained small even for large ϵ and t.) For example, for $\epsilon = 0.8$ and at $t = 50$, the shape difference is about 0.476. A study of the wave profiles reveals the reason for this. As ϵ gets larger, the wave profile for positive time becomes more complex. There are several peaks with different amplitudes in evidence, and each of these propagates at

ϵ	0.5	0.4	0.3	0.2	0.1	0.05	0.025	0.0125
E_2	0.043	0.033	0.024	0.014	0.0051	0.0018	0.00053	0.00015
rate on E_2	1.2	1.1	1.3	1.5	1.5	1.7	1.9	$\to 2$
D_2^s	0.0371	0.0303	0.0230	0.0139	0.00501	0.00173	0.00052	0.00014
rate on D_2^s	0.9	1.0	1.2	1.5	1.5	1.7	1.9	

TABLE 4. The relative L_2 difference and shape difference between solutions $\eta_\epsilon(x,t)$ of (1.1) and $q_\epsilon(x,t)$ of (1.4) at $t=1$, with initial data (4.1) for BBM.

its own speed. As the speeds in the BBM approximation (1.1) are not quite the same as for the Boussinesq approximation (1.4), there is a divergence because of phase differences, just as in Experiment 1. However, because there is substantial energy in more than one wave amplitude, there are several phase differences contributing substantially to the phase mismatch, and no single translation can compensate for them all. To put the issue in simple terms, for given functions f_1 and f_2 one cannot in general obtain a close fit to

$$f_1(x+\alpha_1) + f_2(x+\alpha_2),$$

where α_1 and α_2 are distinct, by using an approximation of the form

$$f_1(x+\alpha) + f_2(x+\alpha).$$

The solutions studied in Experiment 2 also differ from those of Experiment 1 in that their structure changes when ϵ is changed. (In Experiment 1, solutions for all values of ϵ tried had the same structure: namely, that of a solitary wave with a small dispersive tail.) The effects of changing ϵ on the solutions in Experiment 2 may be seen, for example, by comparing the solution for $\epsilon = 0.5$, shown in Figure 3, to that shown in Figure 6, where ϵ has been reduced to 0.05. In Figure 6, where $\eta_\epsilon(x,t)$ is graphed against x for $t = 0$, 10, 20, 30, and 40, it is clear that $\eta_\epsilon(x,t)$ is mainly a right-moving wave. This is in agreement with the result one gets by considering (1.1) to be a perturbation of the linear wave equations

$$\eta_t + v_x = 0$$
$$v_t + \eta_x = 0,$$

with initial conditions $\eta(x,0) = g$ and $v(x,0) = g$. For this reduced system, the exact solution is simply the right-moving wave

$$\eta(x,t) = g(x-t)$$
$$v(x,t) = g(x-t).$$

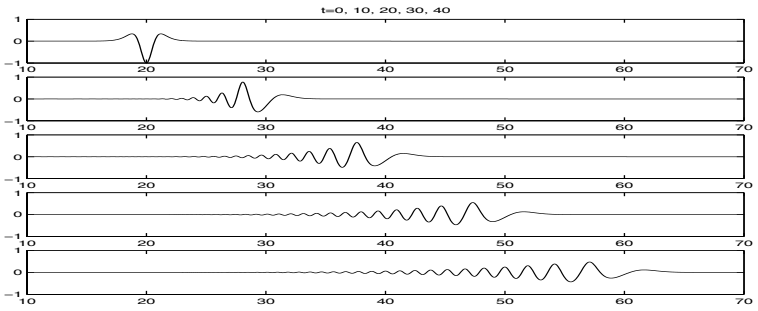

FIGURE 6. Solution of Boussinesq system with $\epsilon = 0.05$.

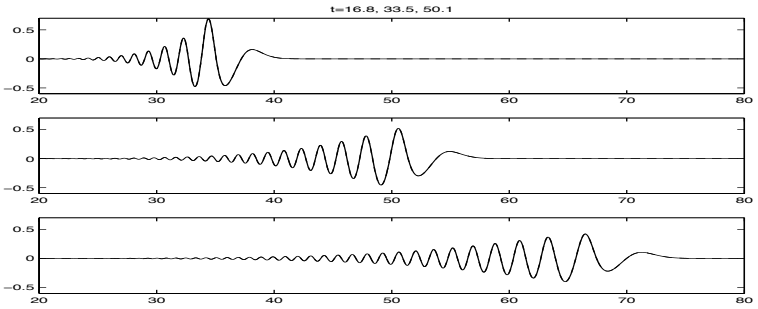

FIGURE 7. Comparison between solutions of BBM equation (solid line) and Boussinesq system (dashed line) with $\epsilon = 0.05$. The difference between the two solutions is not visible.

Comparisons between $\eta_\epsilon(x,t)$ and $q_\epsilon(x,t)$ for $\epsilon = 0.05$ at $t = 16.8$, 33.5, and 50.1 are plotted in Figure 7. The difference between the two solutions is hardly visible. At $t = 50$, the relative difference $E_2(0.05, 50)$ is only 0.009 (see Table 3).

As another check on our code, we monitored the variation of quantities that, for the continuous problem, are independent of time. The integrals

$$I_1(t) = \int_0^L \eta_\epsilon(x,t)\, dx, \quad I_2(t) = \int_0^L v_\epsilon(x,t)\, dx,$$

$$F(t) = \int_0^L \left[\eta_\epsilon v_\epsilon + (\epsilon/6)(\eta_\epsilon)_x (v_\epsilon)_x\right] dx, \quad E(t) = \int_0^L \left[\eta_\epsilon^2 + v_\epsilon^2(1+\epsilon\eta_\epsilon)\right] dx$$

were approximated using the trapezoidal rule. It was found that over the time interval $[0, 50]$, $I_1(t)$ was zero to within 5.9×10^{-6}, $I_2(t)$ stayed within 0.008% of -0.071, $F(t)$ stayed within 0.02% of 0.43, and $E(t)$ stayed within

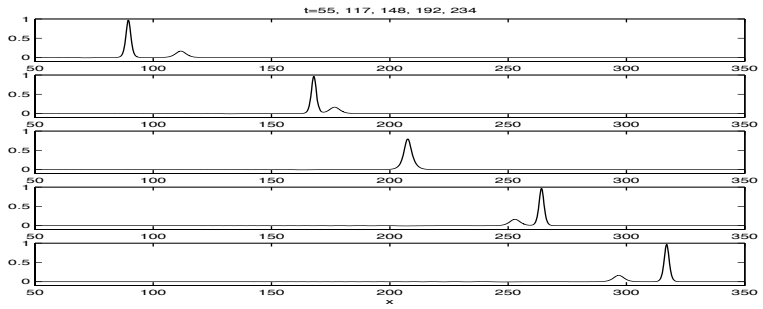

FIGURE 8. Solution of Boussinesq system.

0.000004% of 0.51. Further, all the computations reported here and throughout Section 4 were checked for convergence by halving the spatial and temporal grid lengths and comparing the resulting approximations.

Experiment 3: Solitary-wave interactions. In this experiment, attention is given to the situation wherein a large solitary wave overtakes a smaller solitary wave. The initial data for the BBM equation is the superposition of two exact solitary-wave profiles, namely,

$$q_\epsilon(x,0) = \operatorname{sech}^2\Big(\tfrac{1}{2}\sqrt{\tfrac{3}{1+0.3}}\,(x-20)\Big) + \tfrac{1}{6}\,\operatorname{sech}^2\Big(\tfrac{1}{2}\sqrt{\tfrac{0.5}{1+0.05}}\,(x-54)\Big).$$

Numerical solution of the BBM equation with this type of initial data was carried out earlier in [13]. It was found there that two solitary-wave solutions of the BBM equation do not interact exactly (elastically), as they do in the case of the Korteweg-de Vries equation. From the results of these earlier simulations, we know that it takes a fair amount of time for the two solitary waves to fully interact. Therefore our numerical computation is carried out to $t = 234$.

The surface profiles $\eta_\epsilon(x,t)$ of the solutions of the Boussinesq system (1.1) with $\epsilon = 0.6$ at $t = 55, 117, 148, 192$, and 234 are shown in Figure 8. Notice how closely these profiles resemble those of a double-soliton solution of the Korteweg-de Vries equation. Just as in a Korteweg-de Vries soliton interaction, first the large solitary wave overtakes the smaller one on account of its larger phase speed, then the two waves interact nonlinearly, and finally both emerge from the interaction having regained more or less their original shape and speed. This close resemblance between solutions of (1.1) and the Kortweg-de Vries (or BBM) equation is to be expected, for otherwise the validity of at least one of these models would be in jeopardy. It should be

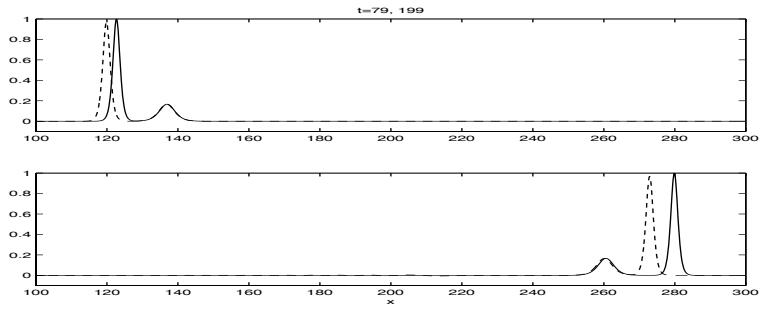

FIGURE 9. Comparison between solutions of BBM equation (solid line) and Boussinesq system (dashed line)

noted, however, that theory still falls short of being able to prove that solutions of (1.1) exhibit the behavior shown in Figure 8 (see [23] for recent work in this direction).

In Figure 9 are shown comparisons between the solutions of the BBM equation (1.4) and the Boussinesq system (1.1), starting from the above initial data, at $t = 79$ and 199. The phase speeds for Boussinesq solitary waves of a given amplitude are smaller than those of the BBM equation. This is especially evident for waves of larger amplitude. At $t = 199$, the phase difference for the large solitary wave has accumulated to the point where the two renditions of it differ by more than one full wavelength.

Experiment 4: Initial-boundary-value problems. In the last experiment, we attempt a simulation that corresponds to waves generated by a wavemaker in a wave tank or to regular, deep-water waves impinging upon a coast. An idealized version of this situation is to pose (1.1) or (1.4) for $(x, t) \in \mathbb{R}^+ \times \mathbb{R}^+$ with zero initial data and a sinusoidal boundary condition

$$q_\epsilon(0, t) = \sin(\pi t) \tanh(5t),$$

which is plotted in Figure 10. The function $\tanh(5t)$ is used to ensure the compatibility of initial data and the boundary data at the corner $(x, t) = (0, 0)$. The left boundary condition for the system (1.1) is taken to be $\eta_\epsilon(0, t) = q_\epsilon(0, t)$ and $v_\epsilon(0, t) = q_\epsilon(0, t) - \frac{1}{4}\epsilon q_\epsilon(0, t)^2$, as in (3.1).

The solutions of the Boussinesq system (dashed line) and the BBM equation (solid line) are plotted in Figure 11 for $\epsilon = 0.2$ and in Figure 12 for $\epsilon = 0.5$. The two solutions have a similar shape, but the waves predicted by the Boussinesq system are smaller and slower than those predicted by the BBM equation. The difference between solutions decreases as ϵ decreases.

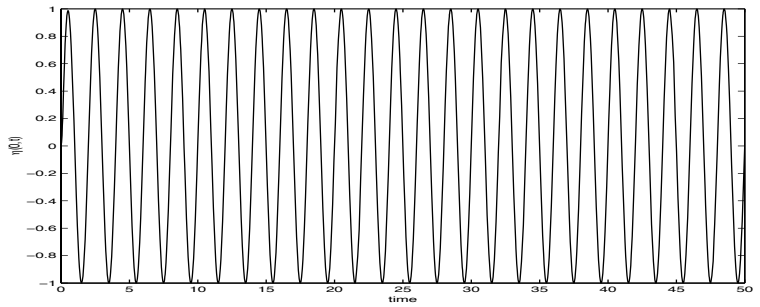

FIGURE 10. Water surface level at the wave maker.

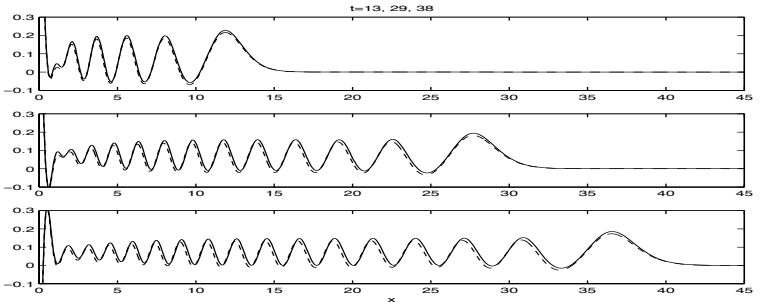

FIGURE 11. Comparison with $\epsilon = 0.2$.

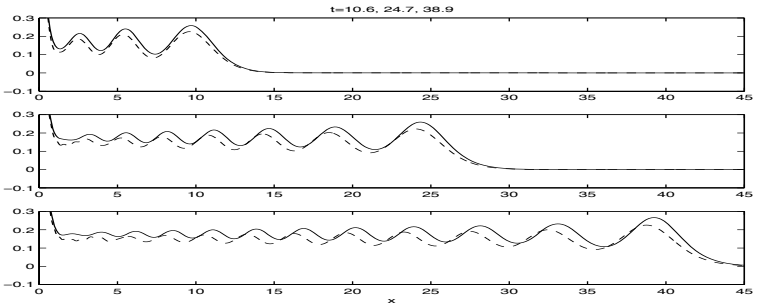

FIGURE 12. Comparison with $\epsilon = 0.5$.

We emphasize that no theory for comparison was developed here for such initial-boundary-value problems, but theory for the individual boundary-value problems can be found in [4], [5], [7], and [12]. Preliminary considerations show that such a theory is not necessarily out of reach, but it is

more complicated than our developments in Section 3 for comparing the pure initial-value problems.

5. Conclusions

When one attempts to model long-crested waves entering the near-shore zone of a large body of water, one naturally aims for the simplest description that is consistent with the accuracy of the input data. On the other hand, most of our knowledge of just how well various modelling approaches work derives from laboratory experiments. In both of these situations, there are available standard unidirectional models such as (1.4) or its variable-coefficient analogues which take account of variable undisturbed depth. These have been shown to predict pretty accurately within their formal range applicability in laboratory environments. There are also available more complicated systems, like (1.1) or its variable-coefficient versions, that can potentially take account of reflection. Our goal here, which had its origins in sediment transport models arising in analyzing beach protection strategies, has been to understand a precise sense in which the bidirectional model specializes to the unidirectional model. This is a fundamental question, but the answer also helps with the formulation of input to the bidirectional model in situations where we would normally have insufficient information with which to initiate the equation. In particular, records of wave-amplitude incoming from deep water are straightforward to use in initiating a unidirectional model like the BBM equation (1.4). As becomes apparent from the analysis in Section 3, the same data can be used to initiate the Boussinesq system (1.1), and with the same implied level of accuracy. The advantage is that the Boussinesq system can countenance reflection whereas (1.1) cannot. Thus, (1.1) can in principle be coupled to models for run-up and reflection in the very-near-shore zone.

In addition to presenting a qualitative theory connected with the comparison of the BBM equation and the Boussinesq system, we have reported numerical experiments showing quantitative aspects of the relation between these two models. After performing convergence tests and the like to generate confidence in our numerical scheme, we ran simulations with initial data corresponding to solitary-wave interactions and to large-scale dispersion. The results show clearly how well the Boussinesq system, with initial velocity as determined from the initial amplitude by (3.2), is tracked by the simple initial-value problem for the BBM equation. Even more convincing are the boundary-value comparisons shown in Experiment 4. As this is an

important context where our ideas could come to the fore, the agreement here is heartening.

Appendix

This appendix contains the proofs of Theorem 3.5 and Lemma 3.10. For the reader's convenience, the results are restated here as Theorems A1 and A2.

Theorem A1. *Let $j \geq 0$ be an integer. Then for every $K > 0$ and every $D > 0$, there exists a constant $C > 0$ depending only on K and D such that the following is true. Suppose $g \in H^{j+5}$ with $\|g\|_{j+5} \leq K$. Let q be the solution of the BBM equation* (1.4) *with initial data $q(x,0) = g(x)$ and let r be the solution of the KdV equation* (1.5) *with initial data $r(x,0) = g(x)$. Then for all $\epsilon \in (0,1]$, if*

$$0 \leq t \leq T = D\epsilon^{-1},$$

then

$$\|q(\cdot,t) - r(\cdot,t)\|_j + \epsilon\|q^2(\cdot,t) - r^2(\cdot,t)\|_j \leq C\epsilon^2 t.$$

Proof. This theorem is essentially proved in [14], to which we refer the reader for details that are omitted here. First consider the case $j = 0$, and let $\theta = q - r$. Then θ satisfies the equation

$$\theta_t + \theta_x + \tfrac{3}{2}\epsilon(r\theta)_x + \tfrac{3}{2}\epsilon\theta\theta_x - \tfrac{1}{6}\epsilon\theta_{xxt} = \epsilon^2 G, \tag{A.1}$$

where $G = -\left(\frac{1}{4}(rr_x)_{xx} + \frac{1}{36}r_{xxxxx}\right)$. Multiplying (A.1) by θ, integrating over $\mathbb{R} \times [0,t]$, and integrating by parts leads to

$$\int_{-\infty}^{\infty} (\theta^2 + \tfrac{1}{6}\epsilon\theta_x^2)\, dx = \tfrac{3}{2}\epsilon \int_0^t r_x\theta^2\, dx\, d\tau + \epsilon^2 \int_0^t \int_{-\infty}^{\infty} G\theta\, dx\, d\tau. \tag{A.2}$$

Now let $A(t) \geq 0$ be defined by setting $A^2(t)$ equal to the integral on the left side of (A.2). It follows easily from (A.2) that

$$A^2(t) \leq C \int_0^t \left[\epsilon^2 A(\tau) + \epsilon A^2(\tau)\right]\, d\tau$$

where C depends only on the norm of r in H^5, and hence, by Lemma 3.10, only on K. By Gronwall's inequality, it then follows that

$$A(t) \leq C_1\epsilon(e^{C_2\epsilon t} - 1)$$

for all $t \geq 0$. In particular, it follows that for any $D > 0$ one can find $C > 0$ such that

$$A(t) \leq C\epsilon^2 t$$

for all $t \in [0, D/\epsilon]$. Thus, for $t \in [0, D/\epsilon]$, we have $\|q - r\|_{L_2} \leq C\epsilon^2 t$, $\|q_x - r_x\|_{L_2} \leq C\epsilon^{3/2} t$, and

$$\begin{aligned}\|q^2 - r^2\|_{L_2} &= \|(q-r)(q+r)\|_{L_2} \leq \|q-r\|_{L_\infty}\|q+r\|_{L_2} \\ &\leq C\|q-r\|_{L_2}^{1/2}\|q_x - r_x\|_{L_2}^{1/2} \leq C(\epsilon^2 t)^{1/2}(\epsilon^{3/2}t)^{1/2} = C\epsilon^{7/4}t.\end{aligned}$$

Therefore,

$$\epsilon\|q^2 - r^2\|_{L_2} \leq C\epsilon^{11/4}t \leq C\epsilon^2 t,$$

as desired.

In case $j \geq 1$, the argument is easier. Starting from (A.1) and following the procedure in Subsection 3.3 above, one obtains that the quantity non-negative $A_j(t)$ defined by

$$A_j^2(t) = \int_{-\infty}^{\infty} \sum_{k=0}^{j} \left[\theta_{(k)}^2 + \frac{1}{6}\epsilon\theta_{(k+1)}^2\right] dx$$

satisfies the estimate

$$A_j(t) \leq C\epsilon^2 t,$$

where C depends only on K. Hence $\|q-r\|_j \leq CA_j(t) \leq C\epsilon^2 t$. In particular, using Lemma 3.10 we have

$$\|q+r\|_j \leq \|q-r\|_j + 2\|r\|_j \leq C\epsilon^2 t + C \leq C$$

for all $t \in [0, D/\epsilon]$, where C depends only on K and D. Since H^j is an algebra for $j \geq 1$, it transpires that

$$\epsilon\|q^2 - r^2\|_j \leq C\epsilon\|q-r\|_j\|q+r\|_j \leq C\epsilon\|q-r\|_j \leq C\epsilon^3 t \leq C\epsilon^2 t,$$

as desired. □

Theorem A2. *Let $s \geq 1$ be an integer. Then for every $K > 0$, there exists $C > 0$ such that the following is true. Suppose $g \in H^s$ with $\|g\|_s \leq K$, and let r be the solution of the KdV equation (1.5) with initial data $r(x,0) = g(x)$. Then for all $\epsilon \in (0,1]$ and all $t \geq 0$,*

$$\|r(\cdot,t)\|_{H^s} \leq C. \tag{A.3}$$

Further, for every integer k such that $1 \leq 3k \leq s$, it is the case that

$$\|\partial_t^k r(\cdot,t)\|_{H^{s-3k}} \leq C.$$

Proof. Define

$$\rho(x,t) = \left(\tfrac{3\epsilon}{2}\right) r(\sqrt{\epsilon/6}(x+t), \sqrt{\epsilon/6}\ t),$$

so that ρ is a solution of the equation

$$\rho_t + \rho\rho_x + \rho_{xxx} = 0. \tag{A.4}$$

As explained in the discussion on [16, pp. 576–578], there exist a countable number of explicitly-defined functionals I_0, I_1, I_2, ... which are, at least formally, conserved under the flow defined by (A.4). As a consequence of the well-posedness theory of KdV presented in [16], one has that in fact $I_k(\rho)$ is independent of time for $0 \le k \le s$, provided $\rho \in H^s$ and $s \ge 2$. This result was later extended to $s \ge 0$ in [18].

Now the functionals I_k are defined on functions $f(x)$ of one real variable by integrals of the form

$$I_k(f) = \int_{-\infty}^{\infty} P_k(f)(x)\ dx,$$

where $P_k(f)$ denotes a polynomial function of f and its derivatives. In fact, $P_k(f)$ consists of a linear combination of monomials

$$(f)^{a_0}\left(\frac{df}{dx}\right)^{a_1}\left(\frac{d^2f}{dx^2}\right)^{a_2}\cdots\left(\frac{d^pf}{dx^p}\right)^{a_p},$$

in which the "rank" of each monomial, defined as $\sum_{i=0}^{p}(1+\frac{1}{2}i)a_i$, is equal to $k+2$. Hence if $\rho(x,t)$ and $r(x,t)$ are viewed as functions of x parameterized by the variable t, we have

$$P_k(\rho)(x,t) = \epsilon^{k+2}\tilde{P}_k(r)(\sqrt{\epsilon/6}(x+t), \sqrt{\epsilon/6}\ t)$$

for all x and t, where $\tilde{P}_k(f)$ denotes another polynomial function of f and its derivatives, which like $P_k(f)$ has coefficients which are independent of ϵ. Now define a functional $\tilde{I}_k$ by the formula

$$\tilde{I}_k(f) = \int_{-\infty}^{\infty} \tilde{P}_k(f)(x)\ dx.$$

Since $I_k(\rho)$ is independent of time, it follows that $\tilde{I}_k(r)$ is independent of time. Then the same argument as used to prove Proposition 6 of [16] allows us to conclude that the norm of r in H^s remains bounded for all time, with a bound which depends only on the H^s norm of $r(x,0) = g(x)$. Notice in particular that since the quantity ϵ does not appear in the definition of the functionals $\tilde{I}_k$, the bound thus obtained is independent of ϵ.

This proves the existence of the desired constant C in (A.3). The desired bounds on the time derivatives of r then follow immediately by using (1.5) to express time derivatives in terms of spatial derivatives. □

References

[1] A. A. Alazman, *A comparison of solutions of a Boussinesq system and the Benjamin-Bona-Mahony equation*, Ph.D. Thesis, Department of Mathematics, University of Oklahoma, Norman, OK (2000).

[2] J. P. Albert and J. L. Bona, *Comparisons between model equations for long waves*, J. Nonlinear Sci., 1 (1991), 345–374.

[3] T. B. Benjamin, J. L. Bona, and J. J. Mahony, *Model equations for long waves in nonlinear dispersive systems*, Philos. Trans. Royal Soc. London, Ser. A, 272 (1972), 47–78.

[4] J. L. Bona and P. J. Bryant, *A mathematical model for long waves generated by wavemakers in non-linear dispersive systems*, Proc. Cambridge Philos. Soc., 73 (1973), 391–405.

[5] J. L. Bona and H. Chen, *Comparison of model equations for small-amplitude long waves*, Nonlinear Anal. TMA, 38 (1999), 625–647.

[6] J. L. Bona and H. Chen, *Solitary waves in nonlinear dispersive systems*, Discrete Contin. Dyn. Syst. Ser. B, 3 (2002), 313–378.

[7] J. L. Bona, H. Chen, S.-M. Sun, and B.-Y. Zhang, *Comparison of quarter-plane and two-point boundary value problems: the BBM-equation*, Discrete Contin. Dyn. Syst., Ser. A, 13 (2005), 921–940.

[8] J. L. Bona and M. Chen, *A Boussinesq system for two-way propagation of nonlinear dispersive waves*, Physica D, 116 (1998), 191–224.

[9] J. L. Bona, M. Chen, and J.-C. Saut, *Boussinesq equations and other systems for small-amplitude long waves in nonlinear dispersive media I: Derivation and the linear theory*, J. Nonlinear Sci., 12 (2002), 283–318.

[10] J. L. Bona, M. Chen, and J.-C. Saut, *Boussinesq equations and other systems for small-amplitude long waves in nonlinear dispersive media II: Nonlinear theory*, Nonlinearity, 17 (2004), 925 – 952.

[11] J. L. Bona, T. Colin, and D. Lannes, *Long wave approximations for water waves*, Arch. Ration. Mech. Anal., (to appear).

[12] J. L. Bona and V. A. Dougalis, *An initial and boundary value problem for a model equation for propagation of long waves*, J. Math. Anal. Appl., 75 (1980), 503–522.

[13] J. L. Bona, W. G. Pritchard, and L. R. Scott, *Solitary-wave interaction*, Phys. Fluids, 23 (1980), 438–441.

[14] J. L. Bona, W. G. Pritchard, and L. R. Scott, *A comparison of solutions of two model equations for long waves*, in Fluid dynamics in astrophysics and geophysics, ed. N. Lebovitz (Chicago, Ill., 1981), vol. 20 of Lectures in Appl. Math., Amer. Math. Soc., Providence, R.I., 1983, 235–267.

[15] J. L. Bona, W. G. Pritchard, and L. R. Scott, *Numerical schemes for a model for nonlinear dispersive waves*, J. Comp. Physics, 60 (1985), 167–186.

[16] J. L. Bona and R. Smith, *The initial-value problem for the Korteweg-de Vries equation*, Philos. Trans. Royal Soc. London, Ser. A, 278 (1975), 555–601.

[17] J. L. Bona and N. Tzvetkov, *Sharp well-posedness results for the BBM-equation*, Preprint, (2002).
[18] J. Bourgain, *Fourier transform restriction phenomena for certain lattice subsets and applications to nonlinear evolution equations. II. The KdV-equation*, Geom. Funct. Anal., 3 (1993), 209–262.
[19] M. Chen, *Solitary wave and multi-pulsed traveling-wave solutions of Boussinesq systems*, Appl. Anal., 75 (2000), 213–240.
[20] J. Colliander, M. Keel, G. Staffilani, H. Takaoka, and T. Tao, *Sharp global well-posedness for KdV and modified KdV on R and T*, J. Amer. Math. Soc., 16 (2003), 705–749.
[21] W. Craig, *An existence theory for water waves, and Boussinesq and Korteweg-de Vries scaling limits*, Comm. PDE, 10 (1985), 787–1003.
[22] J. C. Eilbeck and G. R. McGuire, *Numerical study of the regularized long-wave equation. II. Interaction of solitary waves*, J. Comp. Phys., 23 (1977), 63–73.
[23] K. El Dika and Y. Martel, *Stability of N solitary waves for the generalized BBM equations*, Dyn. Partial Differ. Equ., 1 (2004), 401–437.
[24] C. E. Kenig, G. Ponce, and L. Vega, *A bilinear estimate with applications to the KdV equation*, J. American Math. Soc., 9 (1996), 573–603.
[25] B. Pelloni and V. A. Dougalis, *Numerical solution of some nonlocal, nonlinear dispersive wave equations*, J. Nonlinear Sci., 10 (2000), 1–22.
[26] G. Schneider and C. G. Wayne, *The long-wave limit for the water wave problem. I. The case of zero surface tension*, Comm. Pure Appl. Math., 53 (2000), 1475–1535.
[27] J. F. Toland, *Solitary wave solutions for a model of the two-way propagation of water waves in a channel*, Math. Proc. Cambridge Philos. Soc., 90 (1984) 343–360.
[28] J. F. Toland, *Uniqueness and a priori bounds for certain homoclinic orbits of a Boussinesq system modelling solitary water waves*, Comm. Math. Phys., 94 (1986), 239–254.
[29] J. D. Wright, *Higher order corrections to the KdV approximation for water waves*, Ph.D. Thesis, Department of Mathematics and Statistics, Boston University, Boston, MA (2004).
[30] J. D. Wright, *Corrections to the KdV approximation for water waves*, SIAM J. Math. Anal., (to appear).